Multiplex immunohistochemistry differences between Q fever and atherosclerotic abdominal aortic aneurysms indicate immune suppression

Kimberley R.G. Cortenbach MD[1#], Alexander H.J. Staal MD[1#], Teske Schoffelen[2] MD PhD, Mark A.J. Gorris MSc[1], Lieke L. van der Woude MD[1], Anne F.M. Jansen MD PhD[2], Paul Poyck MD PhD[3], Robert Jan van Suylen MD PhD[4], Peter C. Wever MD PhD[5], Chantal P. Bleeker-Rovers MD PhD[2], Mangala Srinivas PhD[1,6], Konnie M. Hebeda PhD[7], Marcel van Deuren MD[2], Jos W.M. van der Meer MD PhD[2], I. Jolanda M. De Vries PhD[1], Roland R.J. van Kimmenade MD PhD*[8]

[1] Department of Tumor Immunology, Radboud Institute for Molecular Life Sciences, Radboud University Medical Center, Nijmegen, the Netherlands

[2] Department of Internal Medicine, division of Infectious Diseases and Radboud Center for Infectious Diseases, Radboud university medical center, Nijmegen, the Netherlands

[3] Department of Surgery, Radboud University Medical Center, Nijmegen, the Netherlands

[4] Department of Pathology, Pathology DNA, Jeroen Bosch Ziekenhuis, 's Hertogenbosch, the Netherlands

[5] Department of Medical Microbiology and Infection Control, Jeroen Bosch Ziekenhuis, 's Hertogenbosch, the Netherlands

[6] Department of Cell Biology and Immunology, Wageningen University, Wageningen, the Netherlands

[7] Department of Pathology, Radboud University Medical Center, Nijmegen, the Netherlands

[8] Department of Cardiology, Radboud University Medical Center, Nijmegen, the Netherlands

[#] authors contributed equally

* corresponding author

Corresponding author:

Roland van Kimmenade MD PhD

Department of Cardiology route 616

PO Box 9101

6500 HB Nijmegen, the Netherlands

phone:+31 (0)24-361 45 34

fax:+31 (0)24-3635112

email: rolandvank@hotmail.com

Abstract

Background: Chronic Q fever is a zoonosis caused by the bacterium *Coxiella burnetii* which can manifest as infection of an abdominal aortic aneurysm (AAA). Antibiotic therapy often fails, resulting in severe morbidity and high mortality. Whereas previous studies have focused on inflammatory processes in blood, the aim of this study was to investigate local inflammation in aortic tissue.

Methods: Multiplex immunohistochemistry was used to investigate local inflammation in Q fever AAAs compared to atherosclerotic AAAs in aorta tissue specimen. Two six-plex panels were used to study both the innate and adaptive immune system.

Results: Q fever AAAs and atherosclerotic AAAs contained similar numbers of $CD68^+$ macrophages and $CD3^+$ T cells. However, in Q fever AAAs the number of $CD68^+CD206^+$ M2 macrophages was increased, while expression of GM-CSF was decreased compared to atherosclerotic AAAs. Furthermore, Q fever AAAs showed an increase in both the number of $CD8^+$ cytotoxic T cells and $CD3^+FoxP3^+$ regulatory T cells. Lastly, Q fever AAAs did not contain any well-defined granulomas.

Conclusions: These findings demonstrate that despite the presence of pro-inflammatory effector cells, there is an immune suppressive micro environment in Q fever AAA resulting in persistent local infection with *C. burnetii*.

Funding: This work was supported by SCAN consortium: European Research Area - CardioVascular Diseases (ERA-CVD) grant [JTC2017-044] and TTW-NWO open technology grant [STW-14716].

Introduction

Q fever is a zoonosis caused by the Gram-negative intracellular bacterium *Coxiella burnetii (C. burnetii)*, with natural reservoirs in a wide range of wild and domestic animals. In infected animals (such as goats) milk, placenta and birth fluids, can contain this microorganism, which may cause human infections via inhalation. Acute Q fever can present as pneumonia, hepatitis, and isolated fever, yet 60% of cases are asymptomatic. (1) Progression to chronic Q fever occurs in approximately 5% of infected individuals (2); people at risk are older, suffer from renal insufficiency or aneurysm, or previously underwent valvular or vascular prosthesis surgery. (3) Chronic Q fever manifests as endocarditis or vascular Q fever, i.e., infection of an abdominal aortic aneurysm (AAA) or vascular prosthesis. (4-6)

Vascular Q fever has severe clinical consequences. In a population of proven and probable vascular Q fever patients according to the Dutch consensus guideline, a Dutch cohort study has described that complications had occurred in 61% of the cases. Of these complications, acute aneurysms (i.e. rupture, dissection, endoleak or symptomatic aneurysms) were most prevalent (35%), followed by abscesses (22%), and fistula (14%). Moreover, 25% of patients had a definitely or probably chronic Q fever related cause of death. (6) In addition, serological screening of 770 patients with aorto-iliac disease, e.g., aneurysms or previous vascular reconstructions, demonstrated that 16.9% was seropositive for Q fever, of which 30.8% suffered from chronic Q fever. In this group, aneurysm-related acute complications were more common than in aneurysm patients without Q fever. (7)

To elucidate the pathology underlying chronic Q fever, previous studies have mainly focussed on immune responses in peripheral blood. Blood mononuclear cells of patients with chronic Q fever, when exposed to *C. burnetii* in vitro, produce high amounts of Interferon-gamma (IFNg), the

proinflammatory cytokine considered crucial for killing of the pathogen. (8, 9) In the infected tissues, *C. burnetii* resides and replicates in monocytes and macrophages. (10) In vascular Q fever, it is assumed that *C. burnetii* survives in resident macrophages in the vascular wall. (11, 12) In such patients, there is an apparent inability to effectively eradicate *C. burnetii*, despite the aforementioned IFNg response. In general, a pro-inflammatory response with granuloma formation and intracellular killing or control of the bacterium by activated 'M1' monocytes/macrophages is required to contain intracellular infections like Q fever. Surprisingly, the apparent inability of chronic Q fever patients to kill *C. burnetii* has only been investigated in studies *in vitro* which showed suggestive roles for polarization to tolerogenic M2 macrophages and increased numbers of circulating regulatory T cells. (13, 14)

It is still unclear how *C. burnetii* survives and locally escapes the immune system in vascular Q fever. To address this, we have investigated the local immune response in *C. burnetii*-infected AAAs (Q fever AAA), classical atherosclerotic abdominal aortic aneurysms (AAA), acutely infected AAA, and control aorta tissue, using multiplex immunohistochemistry (mIHC). We investigated both the adaptive and innate immune system. We show that in vascular Q fever numerous immune suppressive mechanisms appear to be present, including the absence of pro-inflammatory granulomas, increased numbers of regulatory T cells, polarization of macrophages into the tolerogenic M2 phenotype, and decreased expression of GM-CSF.

Results

Baseline characteristics

This study includes ten Q fever AAAs (with *C. burnetii* PCR positive on aortic tissue), 12 classical atherosclerotic AAAs, two acutely infected AAAs (with positive cultures of Streptococcus species), and five normal abdominal aorta tissues. Table 1 presents baseline characteristics of the cohort, showing that the majority of patients in all groups were males of older age (median 71 years old), and cardiovascular risk factors were common, including hypertension, diabetes mellitus, hypercholesterolemia, and smoking. Additionally, the aortic diameter was similar amongst the groups.

Immune cell activation in Q fever, atherosclerotic, and acutely infected AAAs compared to normal aortas

Our mIHC technique reveals activation of both the innate and the adaptive immune system in Q fever, atherosclerotic, and acutely infected AAAs compared to normal abdominal aortas (Figure 1). In contrast to normal abdominal aortas, both Q fever AAAs and atherosclerotic AAAs showed impressive lymphocyte accumulation and proliferation with very large tertiary lymphoid structures (TLS) present in the adventitial layer (Figure 1F and 1J). Importantly, well-defined granulomas were neither observed in any of the Q fever AAAs, nor in the other groups. In Q fever AAA, elevated numbers of $CD3^+$ T cells (P=0.010) and $CD20^+$ B cells (P=0.012) were observed compared to normal aortas. Atherosclerotic AAAs revealed increased numbers of $CD3^+$ T cells (P=0.005), $CD20^+$ B cells (P=0.003), and $CD15^+$ neutrophils (P=0.023) compared to control. There were no significant differences in the numbers of cells between Q fever AAA and atherosclerotic AAA. As expected, acutely infected AAAs showed an increase in neutrophils compared to normal aortas (P=0.026). Numbers of $CD1c^+$ classical dendritic cell type 2 (cDC2) and $CD68^+$ macrophages were similar among all groups.

The principal component analysis (PCA) demonstrated when using these markers, a clear distinct population with normal aorta samples is formed, whilst the atherosclerotic and Q fever population completely overlapped (Figure 2A). Therefore, we aimed to investigate which markers differ between these two groups. If we add cell subset markers for macrophages and T cells, this overlap has completely disappeared, indicating these subset markers differentiate these groups (Figure 2B). Below, we will elucidate the differences in cell subsets between atherosclerotic AAA and Q fever AAA.

Q fever AAAs show a shift towards M2 macrophages

To investigate whether there are differences in innate immune system activation between atherosclerotic AAA and Q fever AAA, we used mIHC for description of macrophage subset populations based on $CD68^{+}CD206^{-}$ (M1 macrophages) and $CD68^{+}CD206^{+}$ (M2 macrophages) and for expression of matrix metalloproteinase-9 (MMP9) and Granulocyte Macrophage Colony Stimulating Factor (GM-CSF). As demonstrated in Figure 3, CD206 expression colocalized with CD68 in M2 macrophages. We found that in Q fever AAAs, the number of $CD206^{+}$ M2 macrophages was higher than in atherosclerotic aortas (P=0.005)(Figure 3J). These aortas also revealed lower levels of the pro-inflammatory cytokine GM-CSF when corrected for the percentage of macrophages and M2 macrophages (P=0.033 and P=0.007, respectively) (Figure 4). On the other hand, atherosclerotic AAAs showed a larger amount of the more pro-inflammatory $CD206^{-}$ M1 subset compared to Q fever AAAs (P=0.005)(Figure 3J), combined with a higher expression of GM-CSF per macrophage (P=0.033)(Figure 4E). Additionally, we observed a larger $MMP9^{+}$ proportion of macrophages in atherosclerotic AAAs than in Q fever AAAs (P=0.04). These findings are compatible with extensive chronic inflammation but an immune-suppressed environment in Q fever AAAs in contrast to atherosclerotic AAAs.

Increased cytotoxic T cells and regulatory T cells in Q fever AAAs

To study the involvement of the adaptive immune system in both groups, tissues were stained with antibodies against CD8 for cytotoxic T cells, FoxP3 for regulatory T cells, and CD45RO for memory T cells. Helper T cells were defined as $CD3^+$ T cells without CD8 expression.

Whereas the number of $CD3^+$ T cells is equal among vascular Q fever and atherosclerotic AAA samples, samples from patients with vascular Q fever exhibited larger numbers of cytotoxic T cells (P=0.000), coinciding with a decrease of helper T cells (P=0.000) and memory T cells (P=0.023)(Figure 5G). Infiltrates were formed, as depicted by the strong correlation between T- and B-cells (correlation coefficient 0.6 [CI 0.404-0.788], P=0.000).

When correcting numbers of T cell subsets for infiltrate area, we found an increase in the number of cytotoxic T cells in Q fever AAA compared to atherosclerotic AAA (P=0.013)(Figure 5H). If the number of T cell subsets is calculated per mm^2 tissue (defined as entire sample area minus infiltrate area), the numbers of both cytotoxic T cells and regulatory T cells are increased in Q fever AAA (P=0.043 and P=0.036 respectively)(Figure 5I).

Ruptured and non-ruptured aneurysms exhibit similar immune responses

Strikingly, only Q fever AAAs ruptured while the median diameter (60 mm) did not differ from the diameter in the atherosclerotic AAA group (57 mm)(P=0.887). To investigate whether these patients could be included in our analyses, we tested for differences between ruptured (N=3) and non-ruptured (N=21) aneurysms. Although signs of acute inflammation could be expected, no differences were found in the number of T cells (P=0.206), B cells (P=0.407), cDC2 (P=0.150), neutrophils (P=0.275), and macrophages (P=0.176). Also, when testing for cell subsets, ruptured and non-ruptured aneurysms exhibited similar numbers of M1/M2 macrophages (P=0.206), cytotoxic T cells (P=0.329), regulatory T cells (P=0.206), and memory T cells (P=0.176). The similarity of the results between both groups may be explained by the sampling method; all samples were taken from the ventral side of the aneurysm and the rupture side was unknown or not registered at the time.

Q fever aortas reveal extensive fibrosis

All above mentioned features are signs of chronic inflammation and long-existing disease. This was supported by HE- and Elastin Van Gieson (EVG) stainings, which demonstrated destruction of elastin fibers and fibrosis. Both atherosclerotic AAAs and Q fever AAAs exhibited extensive atherosclerotic plaque formation. However, there were large differences in vessel architecture as demonstrated in Figure 6. Earlier studies have extensively described that aortic aneurysms show fragmentation of elastin fibers indicating media degeneration. (15, 16) In our series, the amount of elastin fibers was even more decreased in many Q fever AAAs than in atherosclerotic AAAs with a similar diameter (marked with black arrows). In addition, the tunica adventitia showed extensive fibrosis in Q fever AAAs (marked with asterisks in Figure 6I and 6L). These changes indicate the (more pronounced) disrupted architecture in Q fever AAAs, which can attribute to ongoing inflammation.

Discussion

We are the first to introduce mIHC in vascular Q fever to study ongoing local inflammation. This sophisticated mIHC method enabled us to quantify immune cells in large sections of tissue which minimized sampling bias. First, we showed that granulomas are absent in Q fever AAAs. Second, atherosclerotic and Q fever AAAs were similar when comparing numbers of immune cells. However, there were striking differences in the composition of macrophage- and T cell-phenotypes between AAAs and Q fever AAAs, leading to new insights into the pathogenesis of vascular Q fever and its complications and possibly with therapeutic consequences.

Our first observation, the absence of well-formed granuloma formation in our cohort of Q fever AAAs is an important one, since it suggests that the local immune landscape lacks an adequate pro-inflammatory response. In our series, we could not find any well-formed granuloma similar to how they are described in acute Q fever. In acute Q fever, so called doughnut granulomas are reported: granulomas with a central clear space and a fibrin ring within or at its periphery (1, 17), for example in liver biopsies in case of hepatitis. (18) Here, granuloma is a feature of active defense against the pathogen. This contrasts to chronic Q fever, where granulomas have not been described before. (17, 19) In particular, Lepidi described that resected valve specimens of patients with Q fever endocarditis lacked well-formed granulomas. (12) In vascular Q fever, granulomatous responses consisting of histiocytes surrounding necrotic areas have been reported in Q fever AAAs, however well-formed granulomas were not found. (20) Thus, we would interpret the absence of organized granulomas as the first clue for an immune-suppressed environment in AAA of Q fever patients that allows persisting infection after the acute phase.

Secondly, our results demonstrate some similarities between Q fever AAAs and AAAs. Percentages of $CD3^+$ T cells, $CD20^+$ B cells, $CD1c^+$ cDC2, $CD15^+$ neutrophils, and $CD68^+$ macrophages are similar between the groups with atherosclerotic AAA and Q fever AAA. This finding is supported by the PCA, which shows overlapping populations of atherosclerotic and Q fever AAAs when entering these inflammatory cell markers. This does not come as a surprise since it is well established that vascular Q fever develops in preexisting atherosclerotic aneurysms. (5, 7, 20-22)

Despite the similarities, we discovered that atherosclerotic and Q fever AAAs do have important differences, which emerge when investigating macrophage and T cell subset markers. Macrophages in Q fever AAAs were found to be polarized into the less inflammatory M2 phenotype, which is 'tolerogenic' and poorly microbicidal, in contrast to the M1 phenotype that possesses a machinery that can clear an infection. Interestingly, in the AAAs we found less M2 polarization. This would either indicate that macrophages polarize towards M2 in response to *C. burnetii* infection, or that the presence of M2 polarization is a prerequisite for *C. burnetii* persistence. Previous studies have demonstrated that *C. burnetii* inhabits and proliferates in monocytes and macrophages, and more specifically, in resident vascular wall macrophages in case of vascular Q fever. (10, 12) It has been shown by Benoit et al. that *C. burnetii* stimulates an atypical M2 activation program in monocyte-derived macrophages *in vitro*. (14) M2 polarization of macrophages was also observed in *C. burnetii* infected transgenic mice constitutively expressing IL-10 in macrophage lineage, a mouse model for chronic Q fever pathogenesis. (23) Spleens and livers of these mice showed increased expression of arginase-1 and mannose receptor (CD206) and decreased expression of iNOS, IL-12 and IL-23 in bone-marrow derived macrophages after infection with *C. burnettii* compared to *C. burnetii*-infected wild type mice. These previous findings suggested that chronic Q fever is associated with M2 polarization of macrophages, but direct evidence in chronic Q fever patients was lacking. Our findings

establish that outgrowth and persistence of *C. burnetii* in AAAs is associated with the predominance of M2 macrophages.

There are several possible explanations for the lack of macrophage activation. First, our results demonstrate decreased expression of GM-CSF in Q fever AAAs compared to AAAs. GM-CSF is a pro-inflammatory cytokine that activates granulocytes and macrophages. (24) Its decreased expression in Q fever AAAs may contribute to the immune suppressive environment in Q fever AAA. The role of GM-CSF in the context of aneurysm formation has been investigated previously. (25) Strikingly, Son et al described increased occurrence of aortic dissection and intramural hematoma in wild type mice subjected to aortic inflammation (CaCl2 + Ang II administration) when also receiving GM-CSF. Only administrating GM-CSF, without the prerequisite of aortic inflammation, did not result in aortic dissection or intramural hematoma. Its potential clinical relevance was confirmed in human blood: GM-CSF serum levels of patients suffering from acute dissection were higher than controls with coronary artery disease, aortic aneurysms of healthy volunteers. (25) Additionally, in our cohort we found that Q fever AAAs rupture at smaller diameter compared to atherosclerotic AAA. This finding, combined with the GM-CSF paradox, suggests that the development of Q fever AAAs and atherosclerotic AAAs follow different pathways, however strictly hypothetically.

Second, a key cytokine in activation is IFNg, a T-helper (Th)-1 cytokine that activates macrophages and makes them more microbicidal. Previous studies from our group have demonstrated that peripheral blood mononuclear cells from patients with chronic Q fever exhibit an abundant production of IFNg when exposed to *C. burnetii* antigens. (8, 9) These findings were enigmatic since there is an apparent inability of the patient's immune system to kill *C. burnetii* at the infected sites. The current findings would be compatible with a downregulated IFNg response at the infected site.

In addition to differences in macrophage subsets, differences in T cell subsets were also observed. First, the number of cytotoxic T cells was increased in both infiltrate and surrounding tissue of Q fever AAA compared to AAA. Although the numbers of cytotoxic T cells were high, their function might be compromised, resulting in defective elimination of *C. burnetii*. The increased numbers of regulatory T cells we found in Q fever AAAs may play a role here. An increased number of circulating regulatory T-cells has also been shown by Layez et al in Q fever endocarditis patients and in acute Q fever patients. (13) Regulatory T cells can inhibit cytotoxic T cells directly or indirectly (26), with a possible role for IL-10 produced by this T cell subset. An important role of IL-10 in chronic development of Q fever has been postulated based on converging evidence from a series of *in vitro* studies. IL-10 production by peripheral blood mononuclear cells from patients with Q fever endocarditis and Q fever with valvulopathy who were at risk for developing chronic Q fever was high, compared to control individuals. (27, 28) Moreover, IL-10 specifically increases *C. burnetii* replication in naive monocytes (29) possibly by downregulating IFNg. Finally, low IL-10 production in monocytes from patients with acute Q fever was associated with *C. burnetii* elimination, whereas *C. burnetii* replicated in monocytes from patients with chronic Q fever and high IL-10 production. The microbicidal activity of monocytes from patients with chronic Q fever was restored by neutralizing IL-10. (30) The murine model of chronic Q fever mentioned above, also confirmed a key role for IL-10 in bacterial persistence. *C. burnetii* infection is persistent in mice that overexpress IL-10 in the macrophage compartment. (23) Thus, IL-10 could play a crucial role in this immune-suppressed environment.

The last major difference between Q fever AAA and atherosclerotic AAA is the extent of damage to the vascular wall architecture in Q fever AAAs. This is demonstrated by extensive loss of elastin fibers and increase of fibrosis present in the vascular wall. Fragmentation of elastin fibers has been

described for AAAs previously (16), however we found the loss of elastin fibers more evident in the lesions from Q fever AAAs than atherosclerotic AAAs. Fibrosis is characterized by replacement of normal tissue by excessive connective tissue, and usually follows chronic inflammation. This may be the effect of persistent presence of growth factors, proteolytic enzymes, angiogenic factors, and profibrotic cytokines. (31, 32) Previously, fibrosis was also observed in chronic Q fever endocarditis in humans and cows. (12, 33-35) This indicates that our Q fever AAA cohort suffered from more destructive disease than our AAA cohort.

These novel insights could lead to new clues for novel treatments and thus developments for clinical care. Currently, Q fever AAA still leads to significant morbidity and mortality rates despite antibiotic and surgical treatment. Epidemiological studies demonstrate the similar risk profile of Q fever and non-Q fever infected AAAs, yet the risk of complications is higher in the Q fever infected group (7), even up to 61% (6), and 25% of patients suffering from Q fever AAA had deceased with a definitely/probably chronic Q fever related cause of death. (6) Here, we confirm that in vascular Q fever, the local immune response is skewed towards an immunotolerant state. Hypothetically, the decreased expression of GM-CSF suggests a possible role for immunomodulating treatment, for example with administration of recombinant GM-CSF. This is already approved for neutropenia due to myelosuppression (36), and has been suggested for treatment for pulmonary tuberculosis. (37) There might be a role for immunomodulating adjuvant therapies in patients with Q fever AAA in whom treatment failure is observed with antibiotics alone.

Our study was the first to use mIHC in Q fever AAA and thereby to gain information about the number and proportion of immune cells, and simultaneously obtain spatial information. This powerful technique and the access to rare Q fever AAA tissue are strengths of this study. While other studies have tested for immune cell activation and recruitment in peripheral blood, we were able to

study the actual infected tissue. Interpreting our results in context of previous observations enables us to increase our understanding of the pathophysiology of Q fever AAA. Still, several limitations should be noted. First, our sample size is limited with only ten vascular Q fever samples. However, this is still the largest study investigating local immune responses in Q fever AAA in humans. In addition, in our quantification method we include entire slides up to 238 20x views per patient, which minimizes the effects of the small sample size. Second, consistent with IHC studies in general, we can only describe the immune cells we observe, without answering mechanistic questions. Nevertheless, when interpreting our results in light of the current literature, we can reasonably formulate hypotheses about the pathophysiology and test these in further research.

Taken together, this leads to the following model with a prominent role for immune suppression. First, macrophages that harbor *C. burnetii* are not effectively killing the organisms, probably due to a lack of activation by proinflammatory cytokines like GM-CSF and IFN-g in a microenvironment with excess IL-10. Second, effector T cells that attempt to eliminate the intracellular bacterium residing in monocytes and macrophages, are hindered by regulatory T cells that are prominent IL-10 producers. Third, there is a lack of microbicidal M1 macrophages, instead macrophages are polarized into the tolerogenic M2 phenotype, which leads to insufficient attack of the pathogen, enabling persistent infection.

Methods and materials

Abdominal aorta tissue samples from patients with Q fever infected aneurysms and control groups were investigated with a novel mIHC method to study the involvement of the innate and adaptive immune system in vascular Q fever. The data underlying this article will be shared upon reasonable request to the corresponding author.

Patient samples

Tissue samples were collected from four groups of patients in two Dutch hospitals: Jeroen Bosch Hospitals in 's Hertogenbosch and Radboud university medical center in Nijmegen. The first group consisted of patients diagnosed with *C. burnetii* infected AAA (Q fever AAA) according to the Dutch consensus guideline (38): all patients had an abdominal aneurysm (AAA) and IgG phase I was at least 1:1024 in combination with a positive PCR of aortic tissue. The second group consisted of patients with atherosclerotic atherosclerotic AAA without clinical suspicion of Q fever. The third group consisted of patients with an acutely infected AAA, with the same definition of AAA in combination with positive cultures of *Streptococcus pneumoniae* and *Streptococcus Agalactiae*, respectively. In these three groups AAA was defined as a CT proven abdominal aortic aneurysm with a diameter of at least 3.0 cm. (39) All aneurysmatic tissue samples were either obtained from patients undergoing elective surgical repair or emergency repair in case of aortic rupture. The fourth group consisted of abdominal aorta samples from patients undergoing kidney explantation surgery for transplantation purposes, with an aortic diameter smaller than 3.0 cm. The samples from Jeroen Bosch Hospital were described in a previous study. (20)

The medical ethics committees of the institutions approved the study, in line with the principles outlined in the Declaration of Helsinki (Radboudumc: 2017-3196; Jeroen Bosch Hospital: 2019.05.02.01).

Tissue Processing

During surgery, the ventral part of the abdominal aorta was removed. If necessary, adhering thrombi were gently removed from the tissue before further processing. Directly after collection, samples were fixed in buffered 4% formaldehyde for at least 24 hours and no longer than 72 hours. If large amounts of calcification were present, samples were decalcified by storing them in EDTA solution for another 24 hours. Subsequently, samples were carefully embedded in paraffin in an attempt to include all aorta layers (formalin fixed and paraffin embedded (FFPE)). Of these tissues, full thickness transverse sections of 4 µm were mounted on silane coated glass slides (New Silane III, MUTO PURE CHEMICALS, Japan).

Multiplex Immunohistochemistry

Samples were stained with two mIHC panels, which enclosed the innate and adaptive immune system (Table 2). Optimization and validation of mIHC panels were performed as described previously. (40) Samples were stained with six consecutive tyramide signal amplification (TSA) stains followed by antigen stripping after every staining. This resulted in the fluorophore remaining on the target, thus enabling eight simultaneous colors on one slide (six markers, DAPI and autofluorescence). Slides were stained automatically in a Leica Bond system (BOND-Rx Fully Automated IHC and ISH, Leica Biosystems). After positioning in the machine, slides were deparaffinized, rehydrated and washed with demi water. After this, samples underwent heat induced antigen retrieval (HIER) in BOND Epitope Retrieval 2 (AR9640, Leica Biosystems) or BOND Epitope Retrieval 1 (AR9961, Leica Biosystems) during 20 minutes for the adaptive and innate panel, respectively. Then, protein blocking in Akoya Antibody Diluent/Block (Akoya biosciences, MA) took place for 10 minutes, followed by incubation with the first primary antibody for 1 hour, subsequently with the secondary antibody (Polymer HRP, Ms + Rb (Akoya biosciences, MA)) for 30 minutes and

finally with an Opal fluorophore ((Akoya biosciences, MA) dissolved 1:50 in 1 X Plus Amplification Diluent (Akoya biosciences, MA) for 10 minutes. To facilitate multiplex staining with six markers, samples were heated for 10 minutes which enabled antigen stripping. After this staining cycle, this procedure was repeated for five different primary antibodies, the secondary antibody and corresponding Opal fluorophores. Finally, DAPI was used as a nuclear counterstain and slides were mounted with Fluoromount-G (0100-01; Southern Biotech, Birmingham, AL, USA). All incubations steps were performed at room temperature. Please see Supplementary Table 2 for a more detailed overview of the used reagents.

Imaging, multispectral unmixing and analysis

After staining, image acquisition and immune cell quantification were performed using an automated approach. First, the PerkinElmer Vectra (Vectra 3.0.3; PerkinElmer, MA) scanned whole slides at 4x magnification and 20x magnification, allowing precise cell segmentation incorporating the entire sample. The average 20x views per slide was 283 resulting in an average tissue area of 59.0 ± 32.6 mm^2, and this high number substantially reduces the chance of sampling bias. Spectral libraries and inForm Advanced Image Analysis software (inForm 2.4.8; Akoya biosciences, MA) unmixed these multispectral images (Supplementary Figures 1A and 2A).

Subsequently, inForm Advance Imaging Analysis software was used for segmentation of tissue and cells. For tissue segmentation, tissue slides were divided into tissue, infiltrate, thrombus, blood, and background (Supplementary Figure 1C). This segmentation was based on DAPI, autofluorescence and, if present, also CD20 and CD3. For single cell segmentation, cells were identified with DAPI and autofluorescence, and, depending on the panel, with membrane markers CD20 and CD3 (Supplementary Figure 1B) or CD68, CD206 and CD15. Requiring DAPI for cell segmentation ensured the exclusion of artifact staining, in which DAPI is absent. The output of the software was 20x magnification images and cell data (localization, tissue, phenotype, and marker) per slide. Images

were combined into single flow cytometry standard (fcs) files, allowing analysis in FlowJo (FlowJo 10.0.7, Becton Dickinson, NJ). In FlowJo, only cells in tissue and infiltrate were analyzed and gates were drawn as shown in Supplementary Figure 1E for the adaptive panel and Supplementary Figure 2B for the innate panel by two observers with excellent interobserver correlation (Supplementary Figure 1D and 2D).

These clear distinct positive cell populations were not found for CD45RO and MMP9 as their expression is gradual. (41) For that matter, the gates for these markers were drawn in negative populations, namely non-T cells and non-neutrophils, respectively. Following this, these gates were copied to populations that could express these markers. GM-CSF fcs files did not show distinct positive and negative populations although they were visible at the microscopy images. Therefore, inForm Advance Imaging Analysis software was used for automatically thresholding for GM-CSF per sample, providing the number of GM-CSF positive pixels per sample (Supplementary Figure 2C).

Histology

To study vessel wall architecture, tissue samples were stained with hematoxylin-eosin (HE) and Elastin von Gieson (EVG).

Statistical analysis

SPSS for Windows (IBM Corp, 2017. IBM SPSS Statistics for Windows, Version 25.0. Armonk, NY: IBM Corp) was used for statistical analysis. PRISM 8.0.2 (Graphpad, GSL Biotech LLC, CA) was used for visualization of results. Continuous data were expressed as mean ± standard deviation (SD), or in case of non-Gaussian distribution, as median (interquartile range) (IQR). Kruskal-Wallis test adjusted with Bonferroni correction for multiple testing was used for testing continuous variables between

four groups. Binary variables were tested for differences using the Fisher exact test. Interobserver variability was calculated with the intraclass correlation coefficient (ICC). Correlations between continuous non-Gaussian distributed variables were studied with Kendall's tau because of low numbers per group. $P < 0.05$ was considered statistically significant. Principal component analysis was performed in RStudio 1.2.5033 (RStudio, inc. Boston, MA) and R (R Foundation for Statistical Computing, Vienna, Austria) using singular value decomposition and the tidyverse (42) and factoextra packages. (43)

Acknowledgements

The authors would like to acknowledge Anne van Duffelen and Kiek Verrijp for their help in optimizing the staining procedure, Jelena Meek for assistance in staining, Inge Wortel, Shabaz Sultan, and Johannes Textor for their help in data analysis, and Janneke Timmermans for her feedback. This work was supported by SCAN consortium: European Research Area - CardioVascular Diseases (ERA-CVD) grant [JTC2017-044] and TTW-NWO open technology grant [STW-14716].

Competing interests

None declared.

References

1. Maurin M, Raoult D. Q fever. Clin Microbiol Rev. 1999;12(4):518-53.
2. Fournier PE, Marrie TJ, Raoult D. Diagnosis of Q fever. J Clin Microbiol. 1998;36(7):1823-34.
3. Kampschreur LM, Dekker S, Hagenaars JC, Lestrade PJ, Renders NH, de Jager-Leclercq MG, et al. Identification of risk factors for chronic Q fever, the Netherlands. Emerg Infect Dis. 2012;18(4):563-70.
4. Wegdam-Blans MC, Vainas T, van Sambeek MR, Cuypers PW, Tjhie HT, van Straten AH, et al. Vascular complications of Q-fever infections. Eur J Vasc Endovasc Surg. 2011;42(3):384-92.
5. Botelho-Nevers E, Fournier PE, Richet H, Fenollar F, Lepidi H, Foucault C, et al. Coxiella burnetii infection of aortic aneurysms or vascular grafts: report of 30 new cases and evaluation of outcome. Eur J Clin Microbiol Infect Dis. 2007;26(9):635-40.
6. van Roeden SE, Wever PC, Kampschreur LM, Gruteke P, van der Hoek W, Hoepelman AIM, et al. Chronic Q fever-related complications and mortality: data from a nationwide cohort. Clin Microbiol Infect. 2019;25(11):1390-8.
7. Hagenaars JC, Wever PC, van Petersen AS, Lestrade PJ, de Jager-Leclercq MG, Hermans MH, et al. Estimated prevalence of chronic Q fever among Coxiella burnetii seropositive patients with an abdominal aortic/iliac aneurysm or aorto-iliac reconstruction after a large Dutch Q fever outbreak. J Infect. 2014;69(2):154-60.
8. Schoffelen T, Sprong T, Bleeker-Rovers CP, Wegdam-Blans MC, Ammerdorffer A, Pronk MJ, et al. A combination of interferon-gamma and interleukin-2 production by Coxiella burnetii-stimulated circulating cells discriminates between chronic Q fever and past Q fever. Clin Microbiol Infect. 2014;20(7):642-50.
9. Schoffelen T, Textoris J, Bleeker-Rovers CP, Ben Amara A, van der Meer JW, Netea MG, et al. Intact interferon-γ response against Coxiella burnetii by peripheral blood mononuclear cells in chronic Q fever. Clin Microbiol Infect. 2017;23(3):209.e9-.e15.
10. Ghigo E, Pretat L, Desnues B, Capo C, Raoult D, Mege JL. Intracellular life of Coxiella burnetii in macrophages. Annals of the New York Academy of Sciences. 2009;1166:55-66.
11. Lepidi H, Fournier P-E, Karcher H, Schneider T, Raoult D. Immunohistochemical detection of Coxiella burnetii in an aortic graft. Clinical Microbiology and Infection. 2009;15(s2):171-2.
12. Lepidi H, Houpikian P, Liang Z, Raoult D. Cardiac valves in patients with Q fever endocarditis: microbiological, molecular, and histologic studies. J Infect Dis. 2003;187(7):1097-106.
13. Layez C, Brunet C, Lépolard C, Ghigo E, Capo C, Raoult D, et al. Foxp3(+)CD4(+)CD25(+) regulatory T cells are increased in patients with Coxiella burnetii endocarditis. FEMS Immunol Med Microbiol. 2012;64(1):137-9.
14. Benoit M, Barbarat B, Bernard A, Olive D, Mege JL. Coxiella burnetii, the agent of Q fever, stimulates an atypical M2 activation program in human macrophages. Eur J Immunol. 2008;38(4):1065-70.
15. Jana S, Hu M, Shen M, Kassiri Z. Extracellular matrix, regional heterogeneity of the aorta, and aortic aneurysm. Experimental & Molecular Medicine. 2019;51(12):1-15.
16. Coady MA, Rizzo JA, Goldstein LJ, Elefteriades JA. Natural history, pathogenesis, and etiology of thoracic aortic aneurysms and dissections. Cardiol Clin. 1999;17(4):615-35; vii.
17. Faugaret D, Ben Amara A, Alingrin J, Daumas A, Delaby A, Lépolard C, et al. Granulomatous response to Coxiella burnetii, the agent of Q fever: the lessons from gene expression analysis. Front Cell Infect Microbiol. 2014;4:172-.
18. Pellegrin M, Delsol G, Auvergnat JC, Familiades J, Faure H, Guiu M, et al. Granulomatous hepatitis in Q fever. Hum Pathol. 1980;11(1):51-7.
19. Raoult D, Marrie T, Mege J. Natural history and pathophysiology of Q fever. Lancet Infect Dis. 2005;5(4):219-26.

20. Hagenaars JC, Koning OH, van den Haak RF, Verhoeven BA, Renders NH, Hermans MH, et al. Histological characteristics of the abdominal aortic wall in patients with vascular chronic Q fever. International journal of experimental pathology. 2014;95(4):282-9.
21. Broos PP, Hagenaars JC, Kampschreur LM, Wever PC, Bleeker-Rovers CP, Koning OH, et al. Vascular complications and surgical interventions after world's largest Q fever outbreak. Journal of vascular surgery. 2015;62(5):1273-80.
22. Eldin C, Mélenotte C, Mediannikov O, Ghigo E, Million M, Edouard S, et al. From Q Fever to Coxiella burnetii Infection: a Paradigm Change. Clinical Microbiology Reviews. 2017;30(1):115-90.
23. Meghari S, Bechah Y, Capo C, Lepidi H, Raoult D, Murray PJ, et al. Persistent Coxiella burnetii infection in mice overexpressing IL-10: an efficient model for chronic Q fever pathogenesis. PLoS Pathog. 2008;4(2):e23.
24. Hercus TR, Broughton SE, Ekert PG, Ramshaw HS, Perugini M, Grimbaldeston M, et al. The GM-CSF receptor family: mechanism of activation and implications for disease. Growth factors (Chur, Switzerland). 2012;30(2):63-75.
25. Son B-K, Sawaki D, Tomida S, Fujita D, Aizawa K, Aoki H, et al. Granulocyte macrophage colony-stimulating factor is required for aortic dissection/intramural haematoma. Nature communications. 2015;6:6994.
26. Joosten SA, Ottenhoff TH. Human CD4 and CD8 regulatory T cells in infectious diseases and vaccination. Hum Immunol. 2008;69(11):760-70.
27. Capo C, Zaffran Y, Zugun F, Houpikian P, Raoult D, Mege JL. Production of interleukin-10 and transforming growth factor beta by peripheral blood mononuclear cells in Q fever endocarditis. Infect Immun. 1996;64(10):4143-7.
28. Honstettre A, Imbert G, Ghigo E, Gouriet F, Capo C, Raoult D, et al. Dysregulation of cytokines in acute Q fever: role of interleukin-10 and tumor necrosis factor in chronic evolution of Q fever. J Infect Dis. 2003;187(6):956-62.
29. Ghigo E, Capo C, Raoult D, Mege JL. Interleukin-10 stimulates Coxiella burnetii replication in human monocytes through tumor necrosis factor down-modulation: role in microbicidal defect of Q fever. Infection and immunity. 2001;69(4):2345-52.
30. Ghigo E, Honstettre A, Capo C, Gorvel JP, Raoult D, Mege JL. Link between impaired maturation of phagosomes and defective Coxiella burnetii killing in patients with chronic Q fever. J Infect Dis. 2004;190(10):1767-72.
31. Wynn TA. Cellular and molecular mechanisms of fibrosis. The Journal of pathology. 2008;214(2):199-210.
32. Wynn TA. Common and unique mechanisms regulate fibrosis in various fibroproliferative diseases. The Journal of clinical investigation. 2007;117(3):524-9.
33. Agerholm JS, Jensen TK, Agger JF, Engelsma MY, Roest HI. Presence of Coxiella burnetii DNA in inflamed bovine cardiac valves. BMC Vet Res. 2017;13(1):69.
34. Brouqui P, Dumler JS, Raoult D. Immunohistologic demonstration of Coxiella burnetii in the valves of patients with Q fever endocarditis. Am J Med. 1994;97(5):451-8.
35. De Biase D, Costagliola A, Del Piero F, Di Palo R, Coronati D, Galiero G, et al. Coxiella burnetii in Infertile Dairy Cattle With Chronic Endometritis. Vet Pathol. 2018;55(4):539-42.
36. Dougan M, Dranoff G, Dougan SK. GM-CSF, IL-3, and IL-5 Family of Cytokines: Regulators of Inflammation. Immunity. 2019;50(4):796-811.
37. Damiani G, McCormick TS, Leal LO, Ghannoum MA. Recombinant human granulocyte macrophage-colony stimulating factor expressed in yeast (sargramostim): A potential ally to combat serious infections. Clin Immunol. 2020;210:108292.
38. Kampschreur LM, Wegdam-Blans MCA, Wever PC, Renders NHM, Delsing CE, Sprong T, et al. Chronic Q fever diagnosis— consensus guideline versus expert opinion. Emerging infectious diseases. 2015;21(7):1183-8.
39. Johnston KW, Rutherford RB, Tilson MD, Shah DM, Hollier L, Stanley JC. Suggested standards for reporting on arterial aneurysms. Subcommittee on Reporting Standards for Arterial Aneurysms,

Ad Hoc Committee on Reporting Standards, Society for Vascular Surgery and North American Chapter, International Society for Cardiovascular Surgery. Journal of vascular surgery. 1991;13(3):452-8.

40. Gorris MAJ, Halilovic A, Rabold K, van Duffelen A, Wickramasinghe IN, Verweij D, et al. Eight-Color Multiplex Immunohistochemistry for Simultaneous Detection of Multiple Immune Checkpoint Molecules within the Tumor Microenvironment. J Immunol. 2018;200(1):347-54.

41. Booth NJ, McQuaid AJ, Sobande T, Kissane S, Agius E, Jackson SE, et al. Different Proliferative Potential and Migratory Characteristics of Human CD4⁺ Regulatory T Cells That Express either CD45RA or CD45RO. The Journal of Immunology. 2010;184(8):4317-26.

42. Wickham H, Averick M, Bryan J, Chang W, McGowan L, François R, et al. Welcome to the Tidyverse. Journal of Open Source Software. 2019;4:1686.

43. Alboukadel Kassambara FM. Visualize the Results of Multivariate Data Analyses 2020 [Available from: https://CRAN.R-project.org/package=factoextra.

1 **Figures with corresponding legends**

2

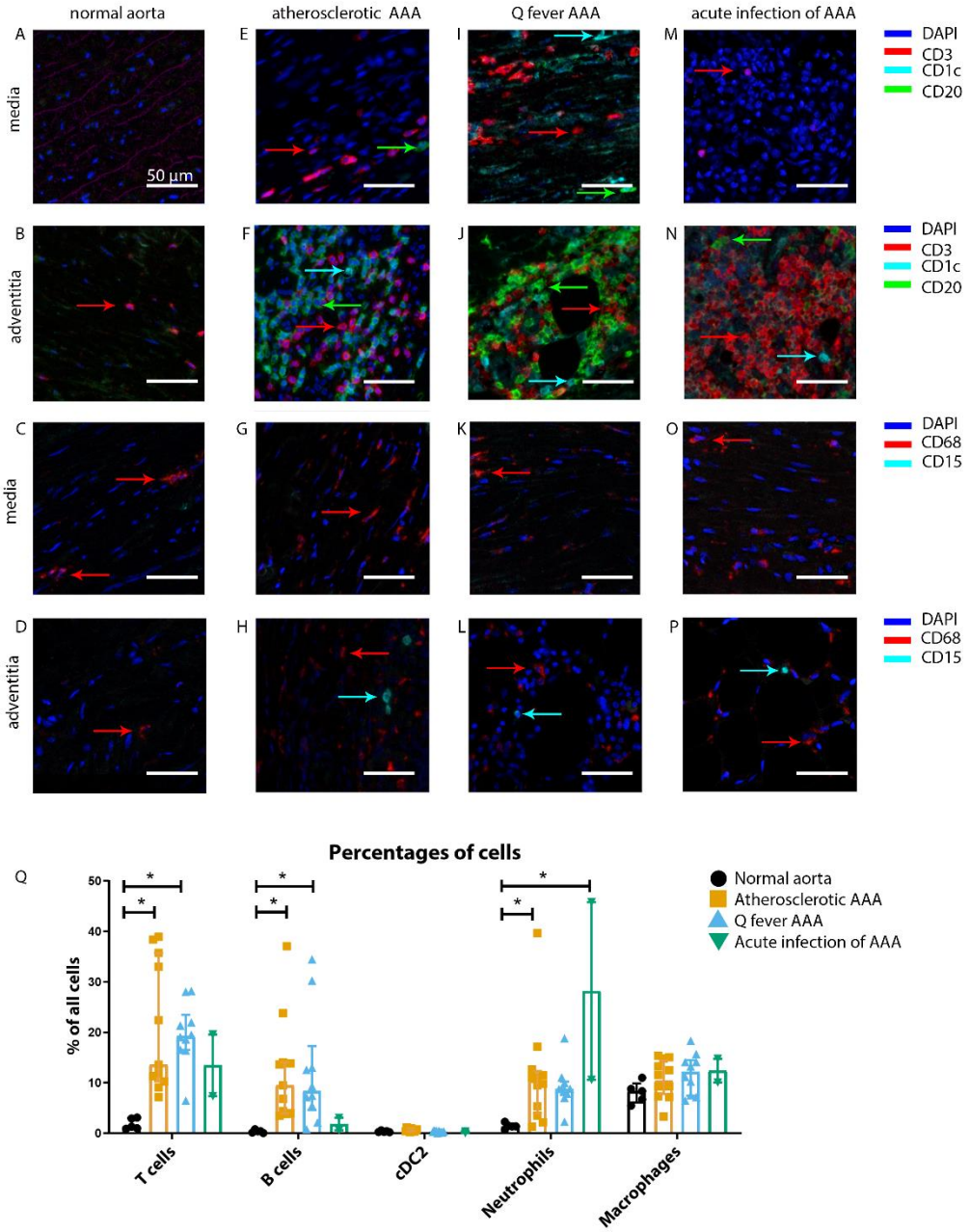

Figure 1: Immune cell activation in atherosclerotic, Q fever infected and acutely infected AAAs. All scale bars represent 50 µm. A-P: Adaptive (A, B, E, F, I, J, M, N) and innate (C, D, G, H, K, L, O, P) immune cells in a representative normal abdominal aorta, atherosclerotic AAA, Q fever AAA and acutely infected AAA. Arrows with corresponding colors indicate presence of immune cells with red for $CD3^+$ T cells, cyan for $CD1c^+$ cDC2, green for $CD20^+$ B cells in the adaptive panel (A, B, E, F, I, J, M, N); and red for $CD68^+$ macrophages and cyan for $CD15^+$ neutrophils in the innate panel (C, D, G, H, K, L, O, P). Q: quantification of percentages of different types of immune cells in the whole tissue sections, showing the increases in T and B cells in atherosclerotic AAA and Q fever AAA compared to normal and increase in neutrophils in acute infection and atherosclerotic AAA compared to normal. Note that there are no differences between atherosclerotic AAA and Q fever AAA. * Represents $P \leq 0.05$.

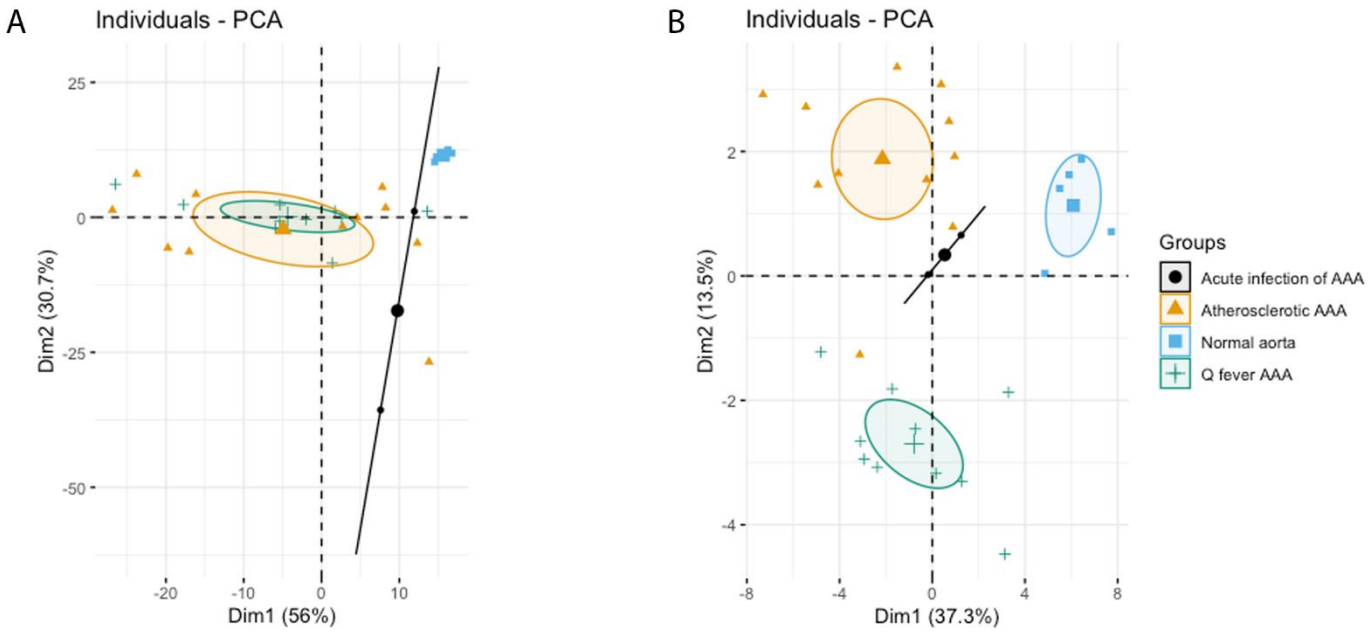

Figure 2: A: Principal component analysis (PCA) including CD3, CD20, CD68, CD15, and CD1c. There is a clear distinct population consisting of normal abdominal aortas. There are two data points for acute infection, resulting in a line. Intriguingly, atherosclerotic AAA and Q fever infected AAA are completely overlapping. This indicates that these populations are similar when testing for these cell markers. B: PCA including all markers (CD68, CD15, MMP9, GMCSF, CD31, CD206, CD3, CD1c, CD8, FoxP3, CD45RO, and CD20). Note the difference with figure 2A: here all groups form separate populations, indicating that the newly added markers including subset markers describe the differences between atherosclerotic and Q fever AAA. See Supplementary Table 1 for loadings of both PCAs.

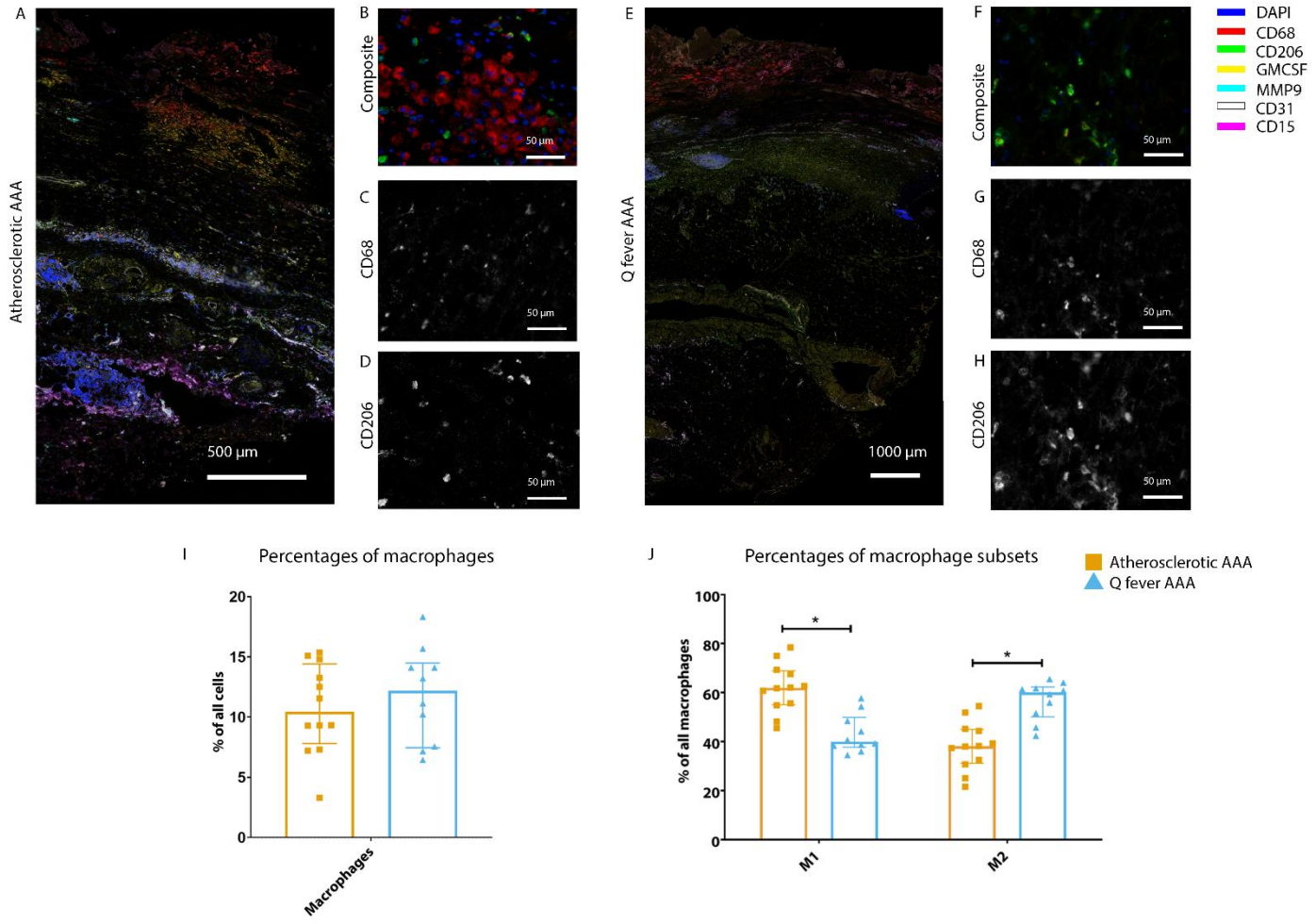

Figure 3: Phenotype shift in macrophages in Q fever towards M2. A: Overview photo of atherosclerotic AAA, upper portion is intima layer, lower portion adventitia. B: Composite of CD68 and CD206 with majority CD68. C, D: Separated channels for CD68 and CD206 respectively. E: Overview of Q fever infected AAA, with the same orientation as A. F: Composite of CD68 and CD206, with mostly CD206+ cells which also express CD68, as supported by separated channels in G and H. I, J: Quantification of percentages of macrophages in entire tissue sections (I) and of proportions of M1 and M2 macrophages in these macrophages (J), showing the phenotype switch in Q fever AAAs towards M2. * Represents $P \leq 0.05$.

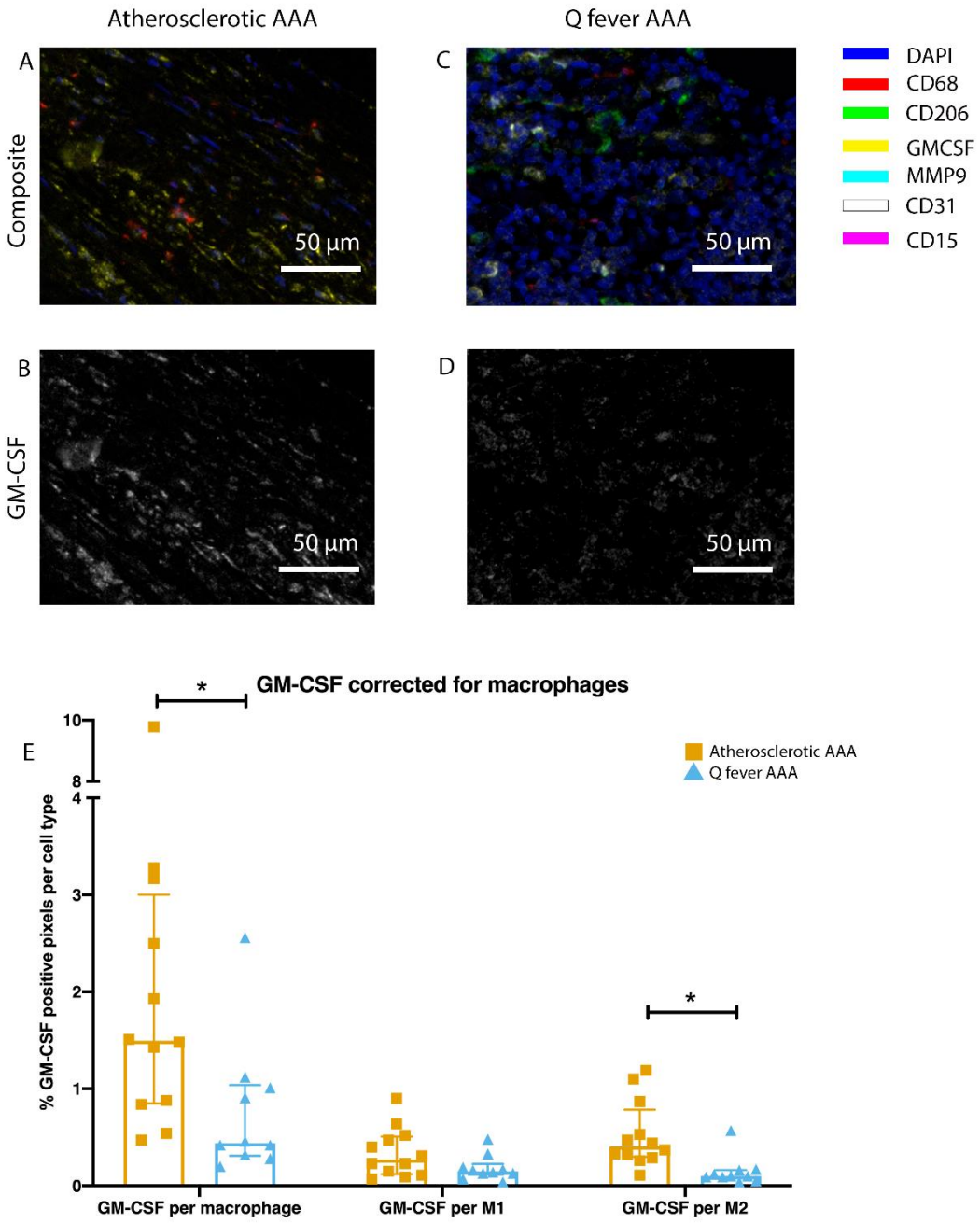

Figure 4: Q fever infected AAAs express lower levels of GM-CSF. A-D: Representative composite image of atherosclerotic AAA (A) and Q fever AAA (C) and corresponding GM-CSF channels (B, D). E: The expressed levels of GM-CSF corrected for the number of macrophages and M2 macrophages are lower in Q fever infected AAAs, suggesting an immune suppressed environment.

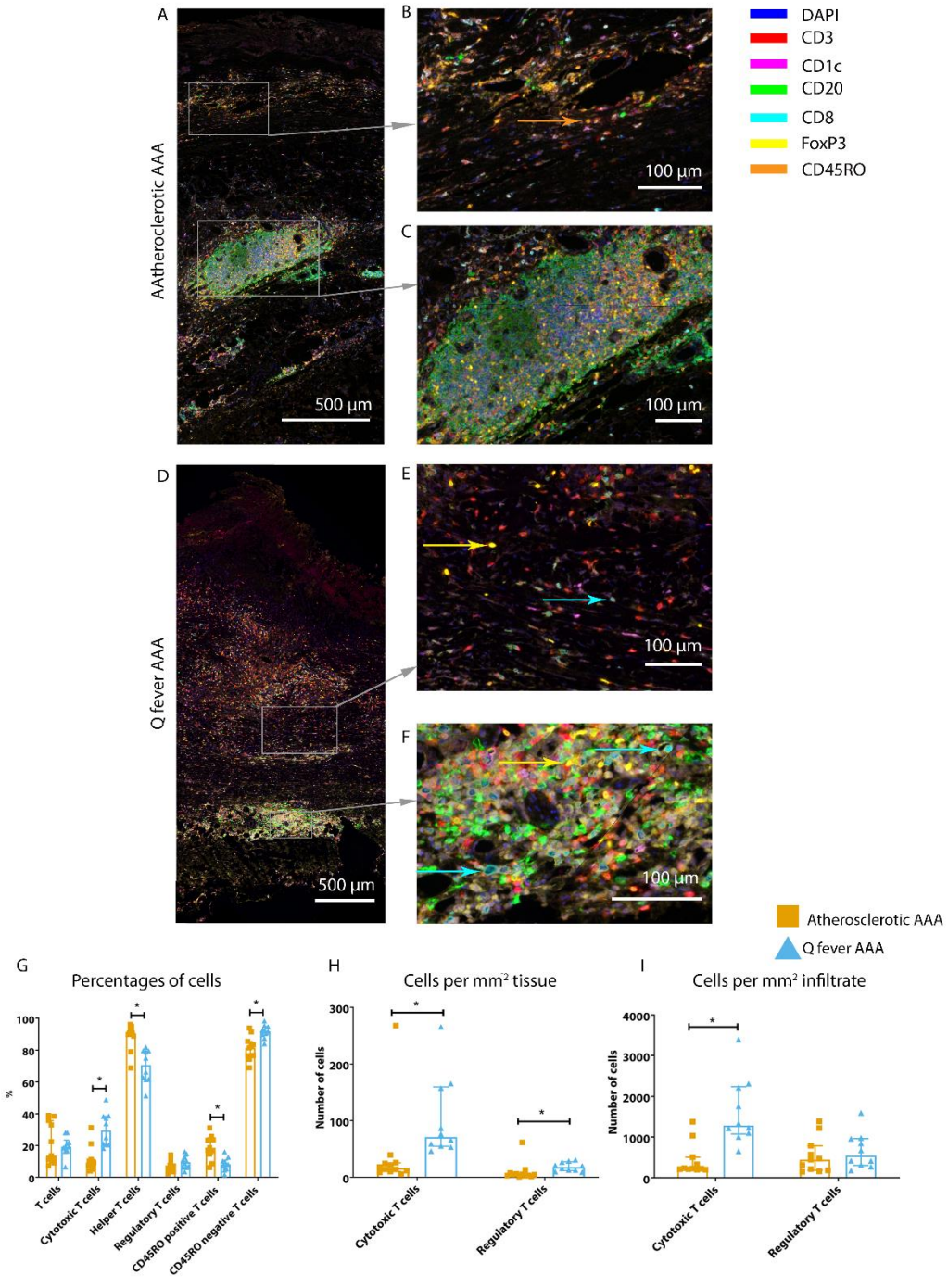

Figure 5: Q fever AAAs exhibit both pro-inflammatory and anti-inflammatory T cell subsets. Arrows with corresponding colors indicate presence of immune cells, with orange for memory T cells, yellow for T helper cells, and cyane for cytotoxic T cells. A-F: Overview of atherosclerotic AAA (A) and Q fever AAA with zoomed photos of tissue (B, E) and tertiary lymphoid structures (TLS)(C, F). In both A and B the upper side of the photo is the intima layer. Note all the FoxP3+ (yellow) cells in Q fever infected tissue. G: Percentage of T cells of all cells and T cells subsets out of T cells; G, H, I: Quantification shows a shift in cytotoxic / helper T cell ratio and decrease in memory T cells in Q fever AAAs. Q fever AAAs show increased numbers of cytotoxic and regulatory T cells, indicating both immune activation and suppression.

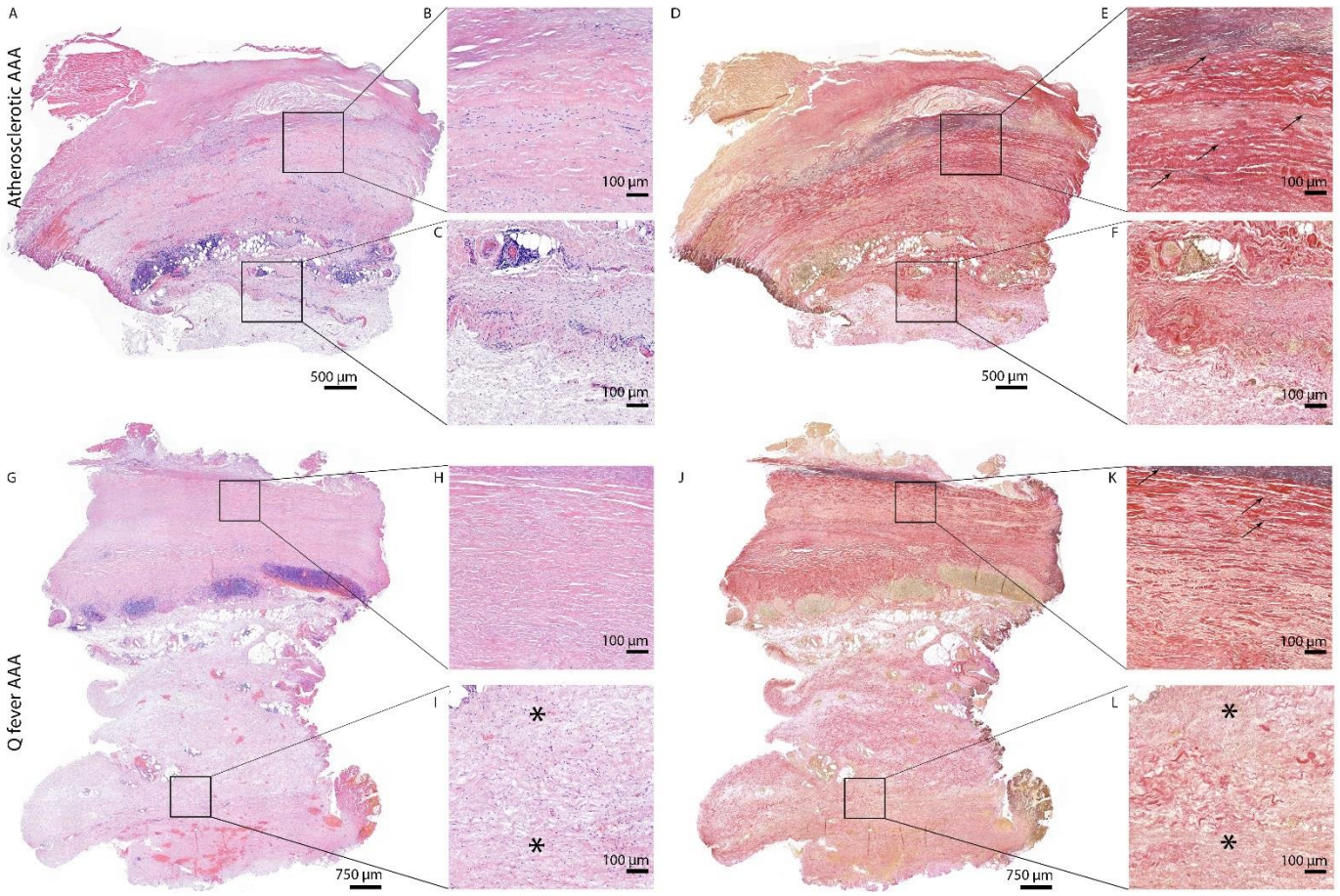

Figure 6: HE and Elastin von Gieson (EVG) stainings demonstrate the disrupted architecture of Q fever infected AAAs. Representative images of HE staining of AAA with 22x zoomed in sections (A, B, C) and EVG staining of adjacent slide (D, E, F) demonstrate the atherosclerotic plaque, immune cells and infiltrates with relatively preserved vessel architecture as shown by presence of elastin fibers (black arrows pointing at black lines). HE (G, H, I) and EVG (J, K, L) of adjacent Q fever AAAs slides reveal pronounced atherosclerosis and immune cell infiltration, and loss of elastin fibers in the media layer (K). In the adventitia (I, L) tissue is replaced by large amounts of fibrosis, indicated with asterisks.

Tables

Characteristic	Normal (N=5)	Missing data normal	Atherosclerotic AAA (N=12)	Missing data atherosclerotic	Q fever AAA (N=10)	Missing data Q fever	Infectious AAA (N=2)	Missing data infectious	Significance
Male	3 (60%)	2	10 (83.3%)	0	9 (90.0%)	1	1 (50.0%)	1	0.482
Age	65 (54-68)	0	72 (66-78)	0	71 (64-77)	0	71 (71-71)	1	0.318
Length	1.80 (1.69-1.83)	0	1.77 (1.69-1.80)	0	1.78 (1.70-)	8	1.76-1.76-1.76)	1	0.923
Weight	80.0 (77.5-102.5)	0	82.6 (75.5-92.6)	0	88.5 (79-)	8	94.8 (94.8-94.8)	1	0.637
BMI	27.0 (22.1-34.7)	0	26.8 (24.0-29.4)	0	27.8 (27.3-)	8	30.6 (30.6-30.6)	1	0.651
Hypertension	3 (60%)	0	8 (66.7%)	0	6 (60.0%)	2	1 (50.0%)	1	1.000
Hypercholesterolemia		5	9 (75.0%)	0	6 (60.0%)	2	0 (0.0%)	1	0.426
DM	1 (20%)	0	3 (25.0%)	0	1 (10.0%)	2	0 (0.0%)	1	0.853
Total cholesterol		5	3.6 (3.0-5.2)	5	4.7 (3.2-6.1)	5		2	0.371
HDL		5	0.9 (0.8-1.1)	6	0.9 (0.9-1.3)	5		2	0.583
Previous aorta surgery	0 (0.0%)	0	6 (50.0%)	0	0 (0.0%)		0 (0.0%)	1	0.034*
Rupture	0 (0.0%)	0	0 (0.0%)	0	3 (30.0%)	0	0 (0.0%)	0	0.193
Artery disease	1 (20%)	4	11 (91.7%)	0	4 (40.0%)	2	1 (50.0%)	1	0.002*
Smoking	3 (60%)	5	11 (91.7%)	1	6 (60.0%)	1	1 (50.0%)	1	0.387
Packyears	27 (27-27)	4	33 (20-50)	2	45 (0-53)	1	0 (0-0)	1	0.819
CRP		5		12	12.5 (12.0-65)	4		2	n/a
Diameter CT		5	57 (55-71)	0	60 (45-81)	1	46 (46-46)	1	0.397
Beta blocker	1 (20%)	3	8 (66.7%)	0	3 (30.0%)	2	0 (0.0%)	1	0.567
ARB / ACEi	2 (40%)	2	6 (50.0%)	0	3 (30.0%)	2	0 (0.0%)	1	0.789
Calciumblocker	0 (0%)	3	3 (25.0%)	0	0 (0.0%)	2	0 (0.0%)	1	0.439
Diuretics	0 (0%)	4	1 (8.3%)	0	2 (20.0%)	0	1 (50.0%)	1	0.009*

1 Table 1: Baseline characteristics. * Represents $P \leq 0.05$. Numbers display numbers of patients with percentage, or median with interquartile range (IQR).

2

	Adaptive immune system		Innate immune system	
Markers (clone)	DAPI		DAPI	
	CD3 (SP7)		CD68 (PG-M1)	
	CD8 (CD8/144B)		CD206 (CL038+)	
	CD20 (L26)		CD15 (MMA)	
	CD1c (2F4)		CD31 (JC70A)	
	FoxP3 (236A/E7)		MMP9 (polyclonal)	
	CD45RO (UCHL-1)		GM-CSF (polyclonal)	
	Autofluorescence		Autofluorescence	
Cell phenotype	T cell	CD3+	Macrophage	CD68+
	Helper T cell	CD3+ CD8-	M1-like macrophage	CD68+ CD206-
	Cytotoxic T cell	CD3+ CD8+	M2-like macrophage	CD68+ CD206+
	Regulatory T cell	CD3+ CD8- FoxP3+	Neutrophil	CD15+
	Memory T cell	CD3+ CD45RO+	Endothelium	CD31+
	B cell	CD20+	MMP9+ cell	MMP9+ CD15-
	Classic DC type 2	CD1c+ CD20-	MMP9+ neutrophil	MMP9+ CD15+
	DAPI	Nucleus	DAPI	Nucleus
	Autofluoresence	Elastin fibers	Autofluoresence	Elastin fibers

1

2 Table 2: Overview of the used markers and clones per panel, including definition of each cell type as used for our analysis.

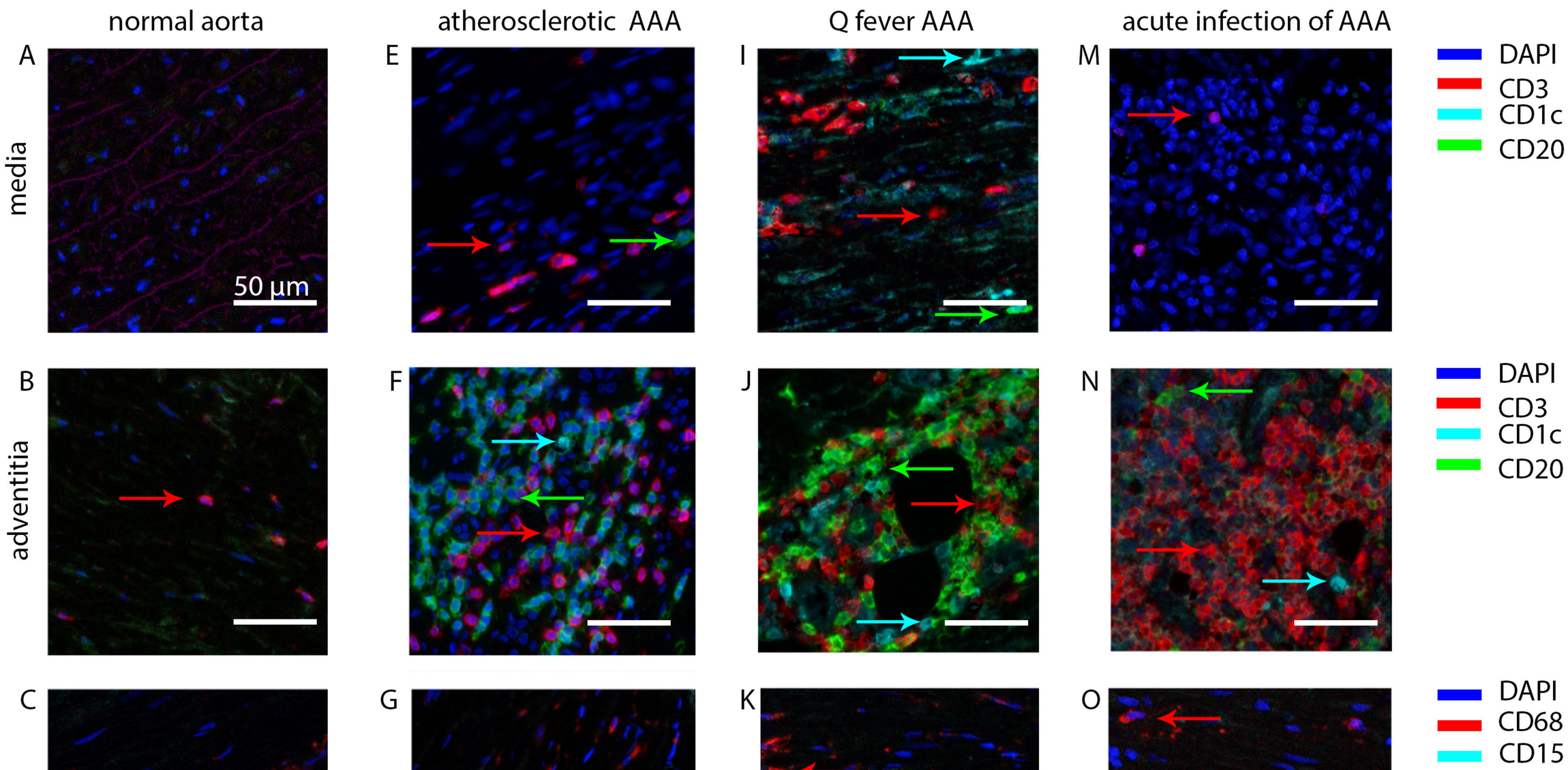

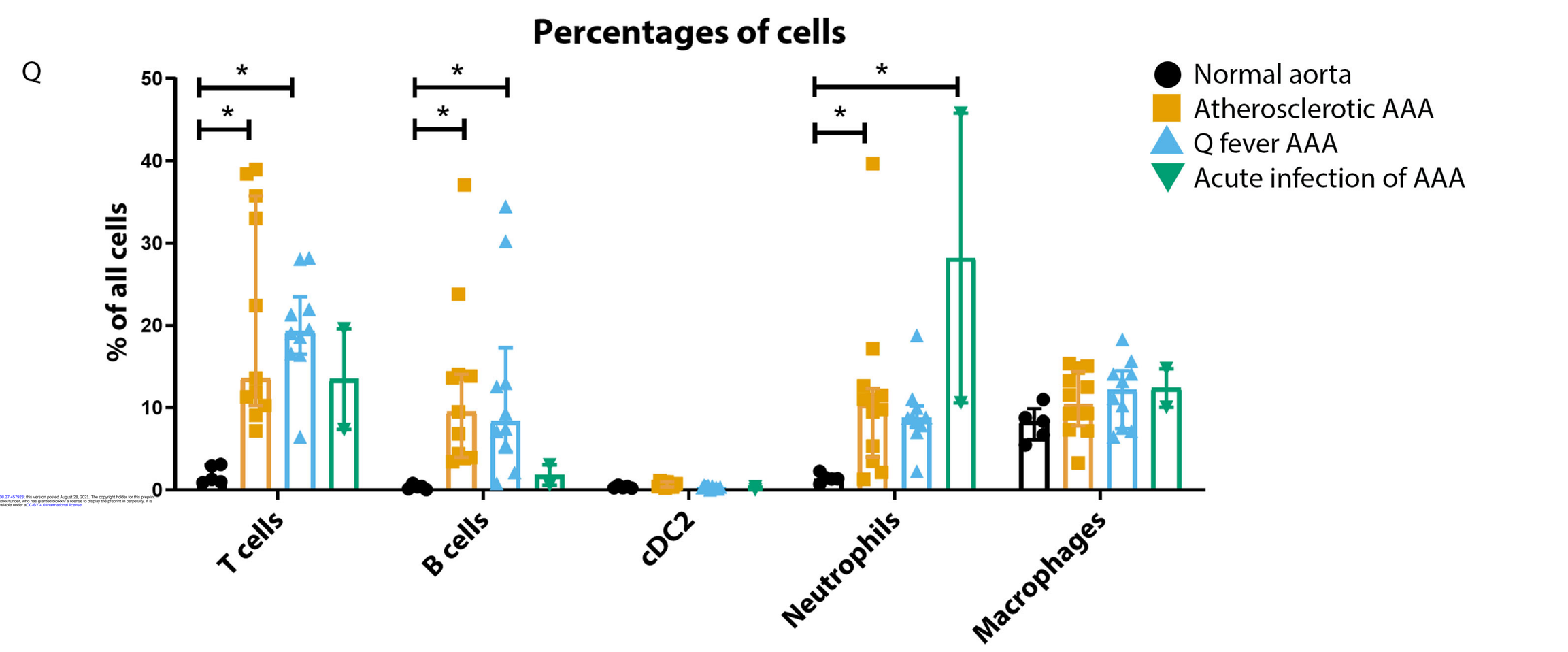

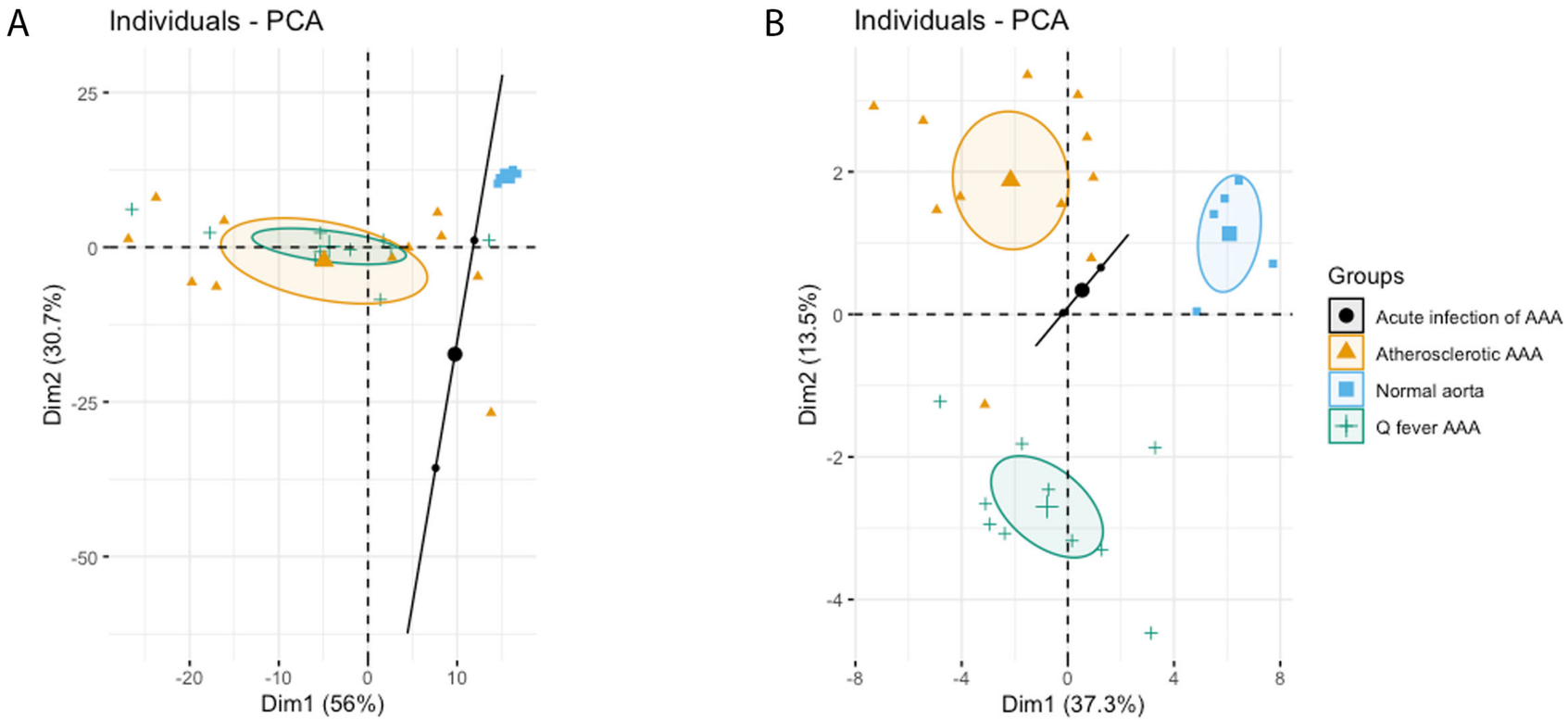

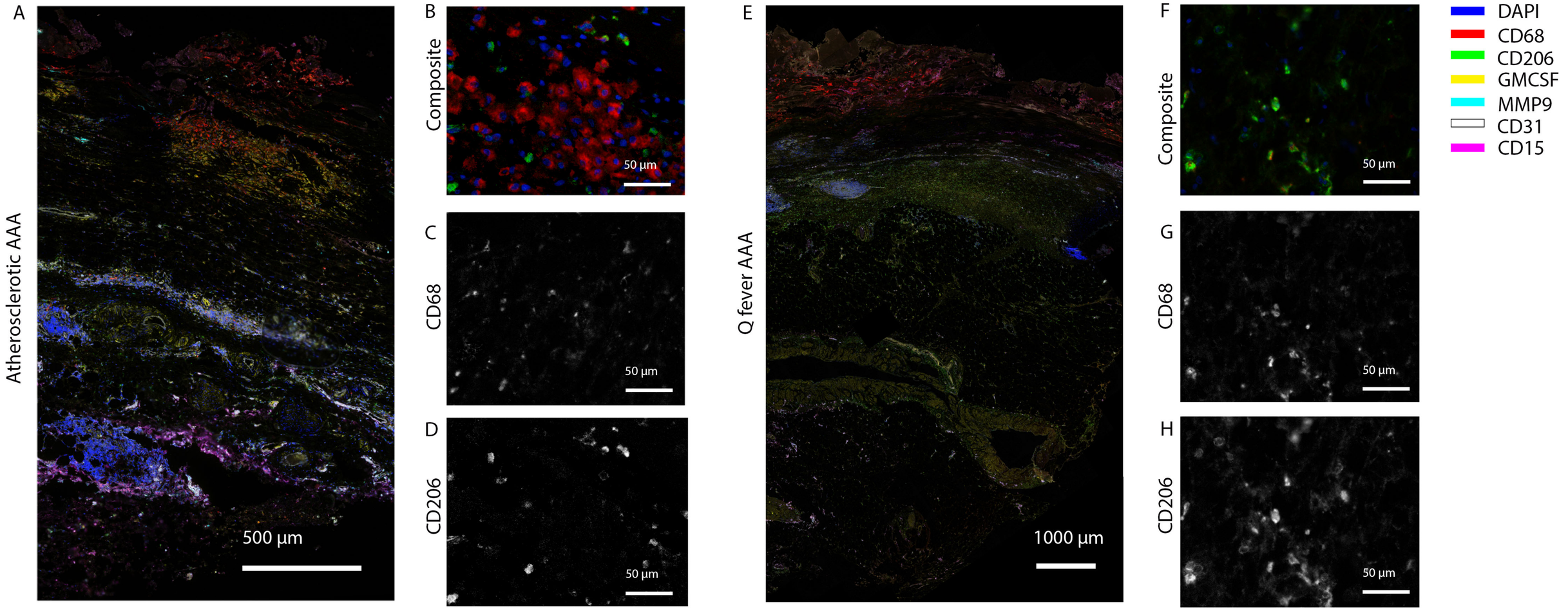

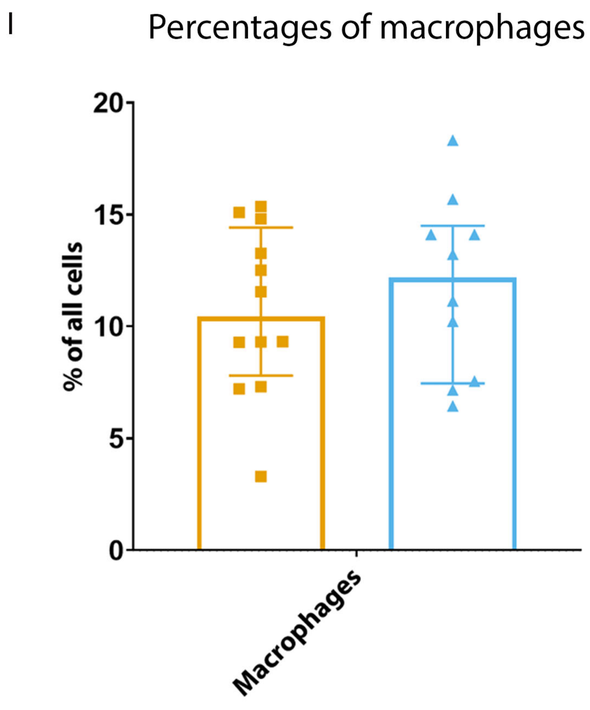

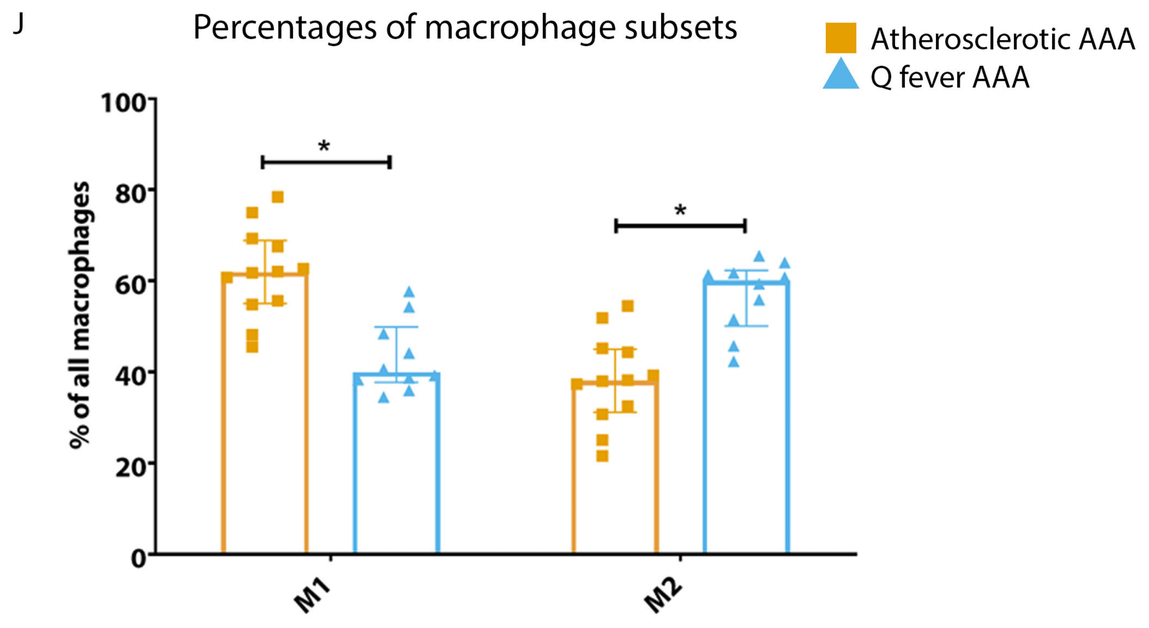

Atherosclerotic AAA

Q fever AAA

A

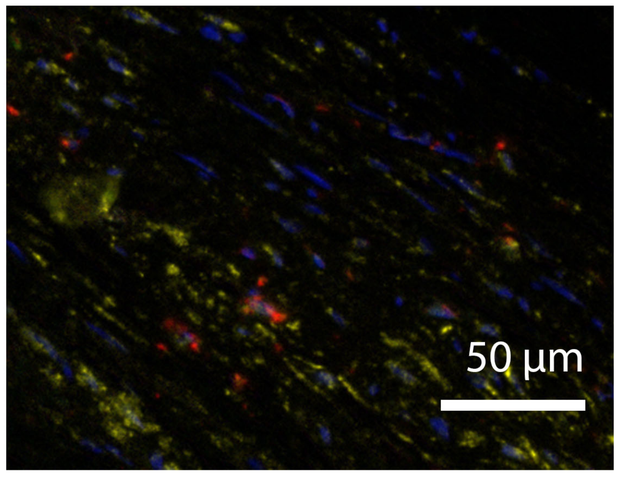

C

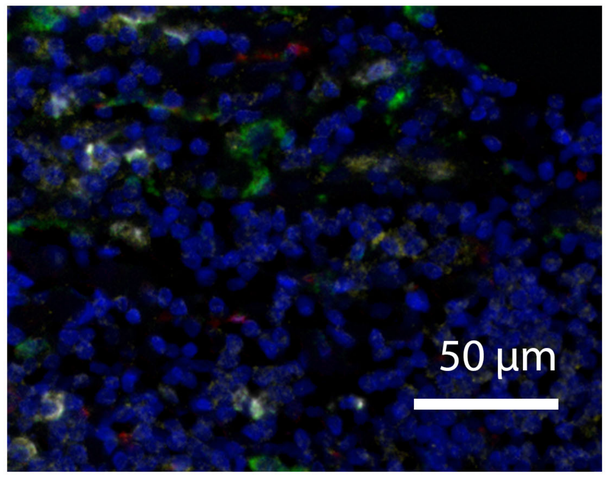

DAPI
CD68
CD206
GMCSF
MMP9
CD31
CD15

Composite

B

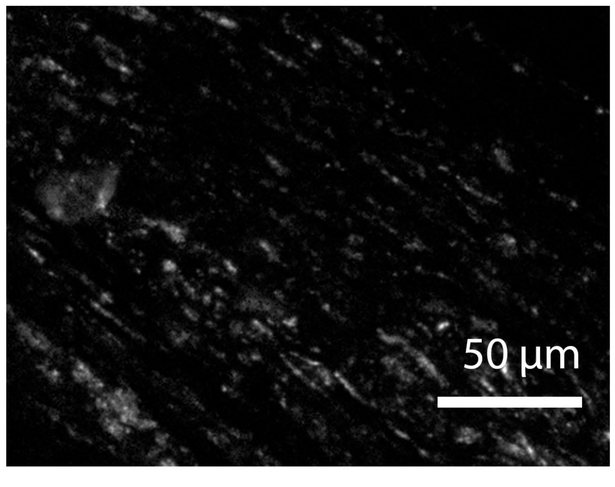

D

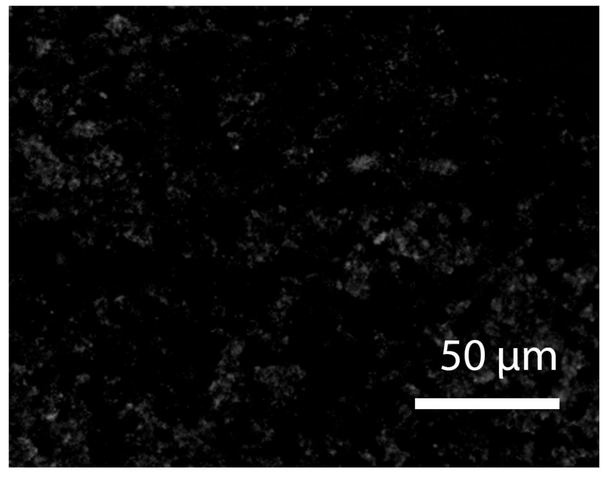

GM-CSF

E

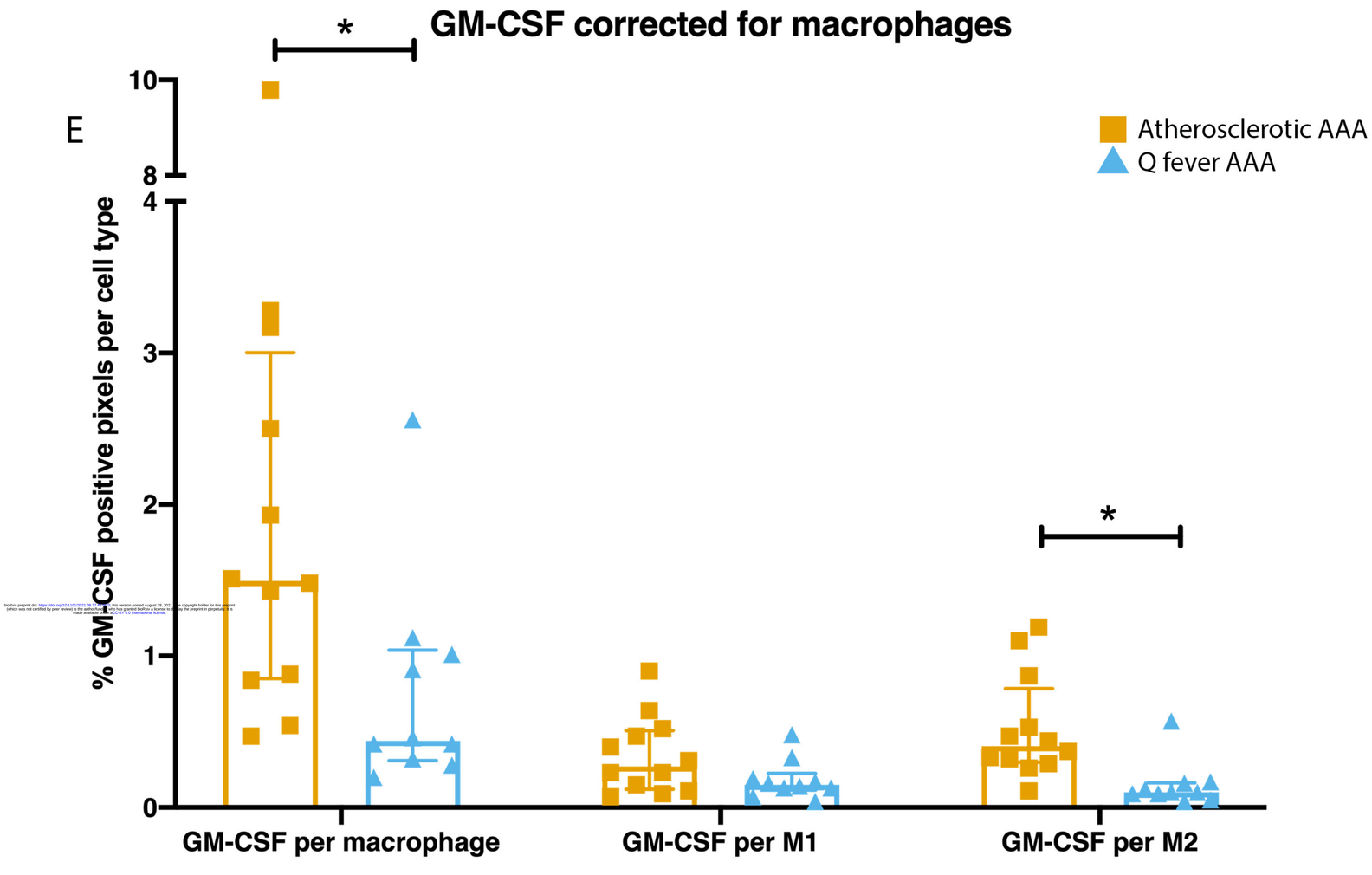

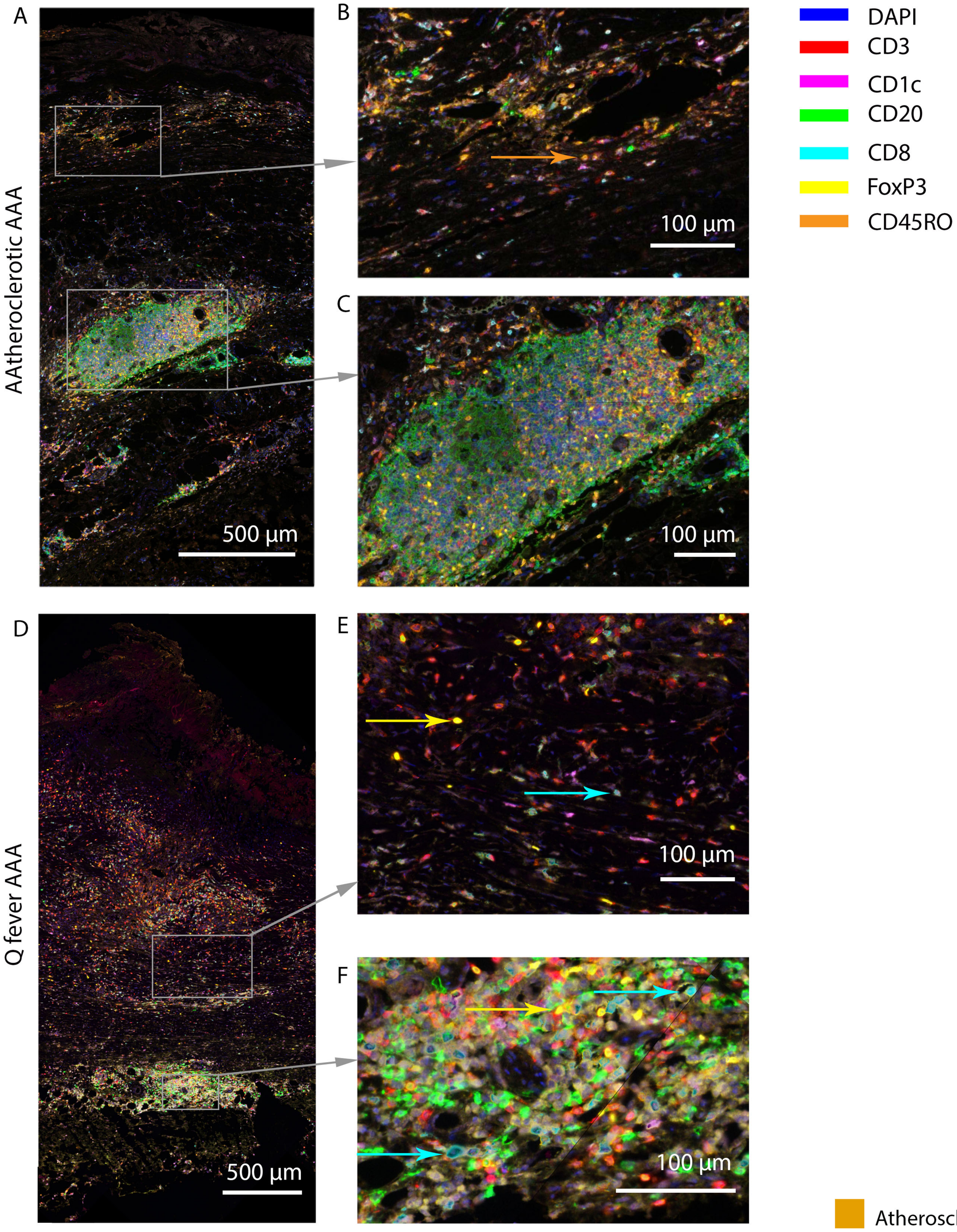

G

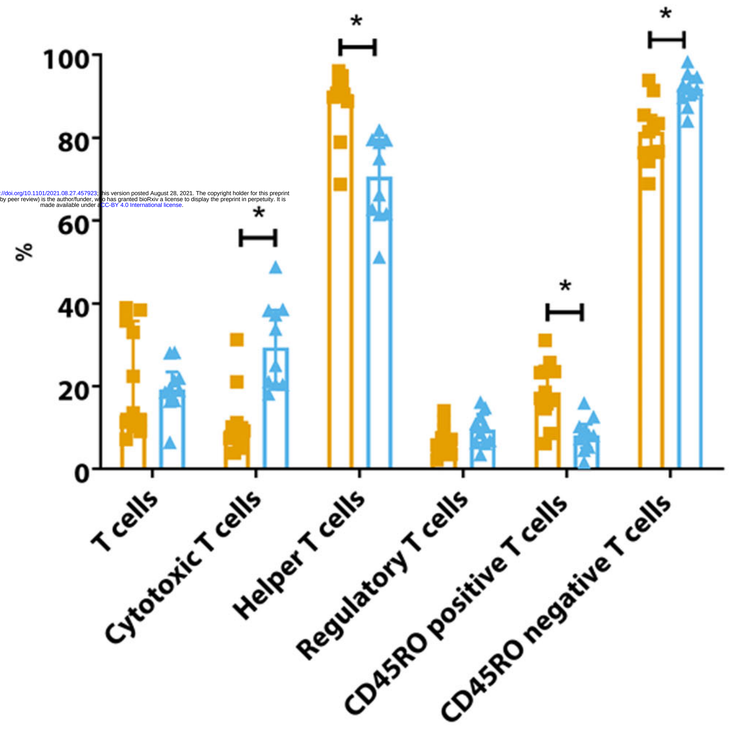

H

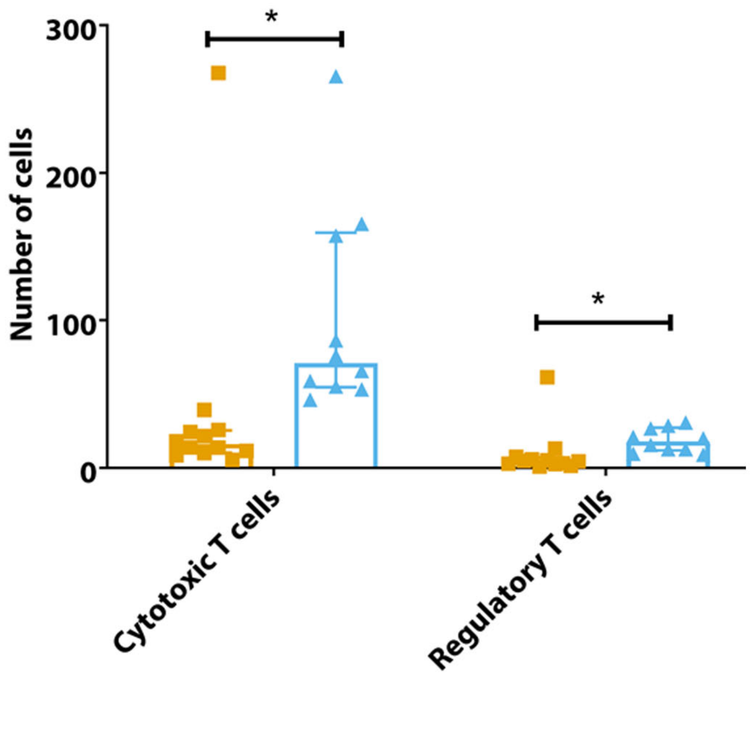

I

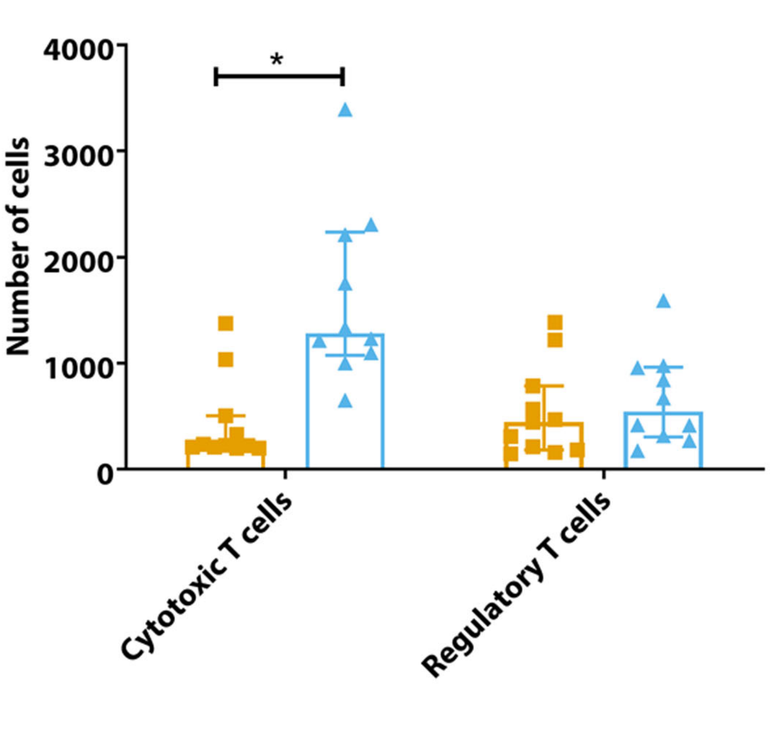

Atherosclerotic AAA

A

B

100 µm

C

500 µm

100 µm

D

E

100 µm

F

500 µm

100 µm

Q fever AAA

G

H

100 µm

I

750 µm

100 µm

J

K

100 µm

L

750 µm

100 µm

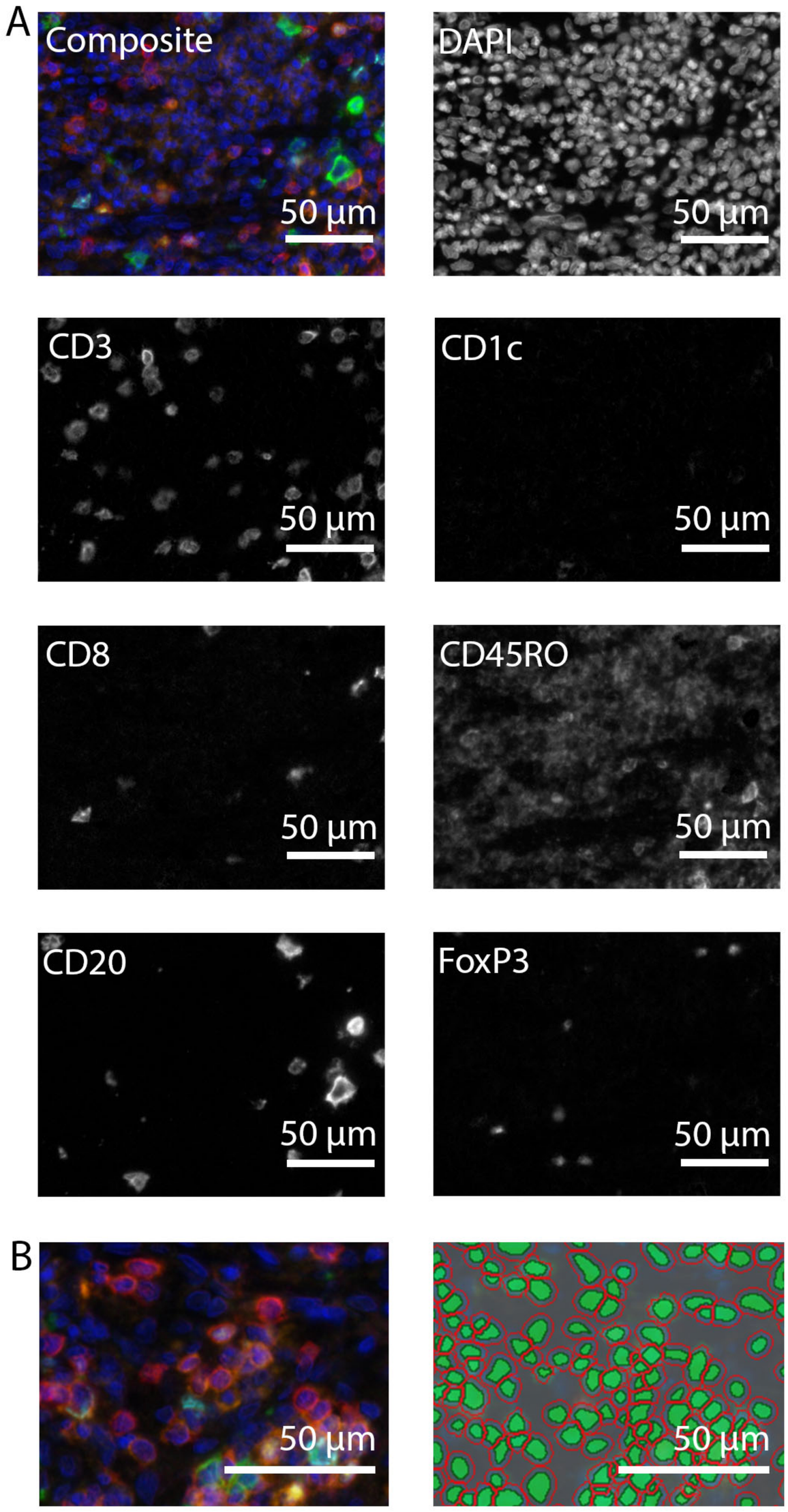

A

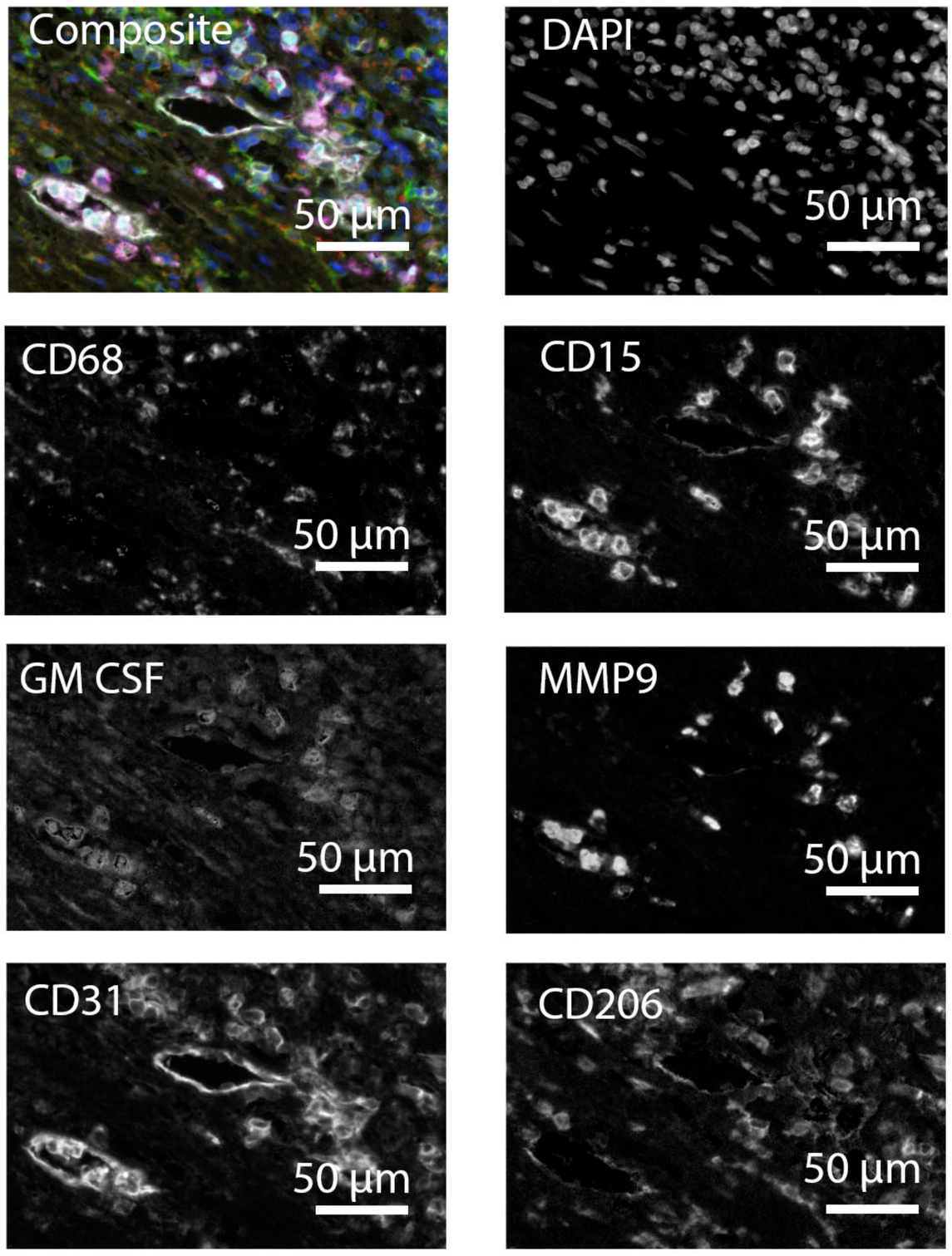

C

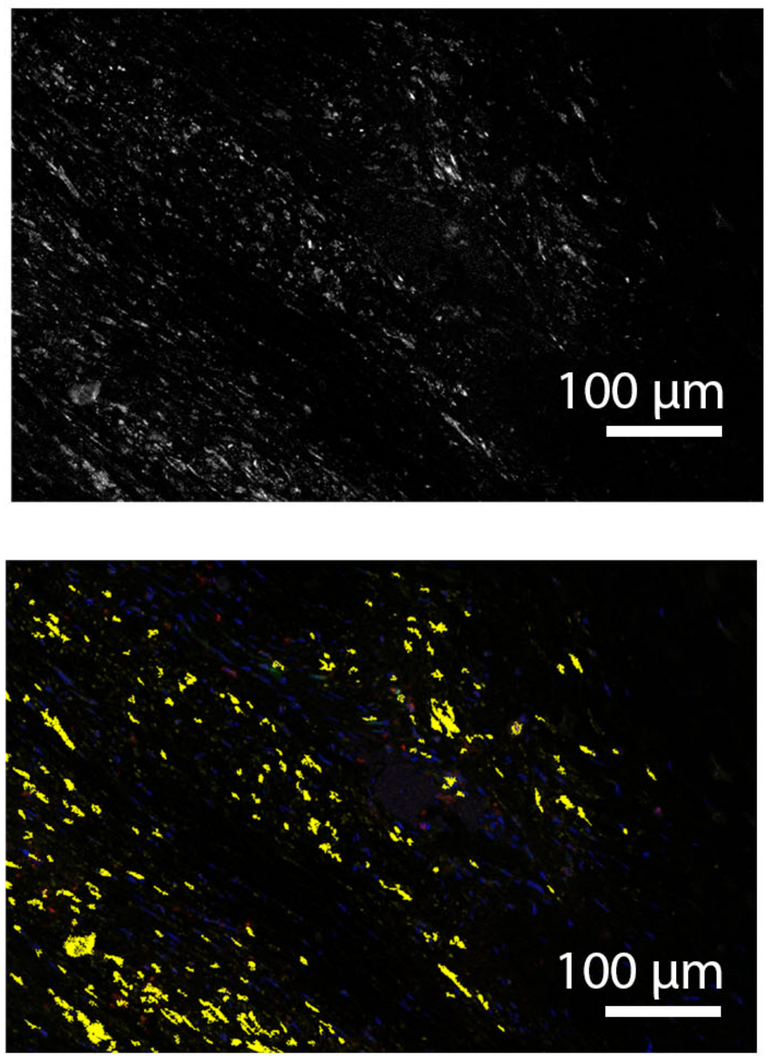

B

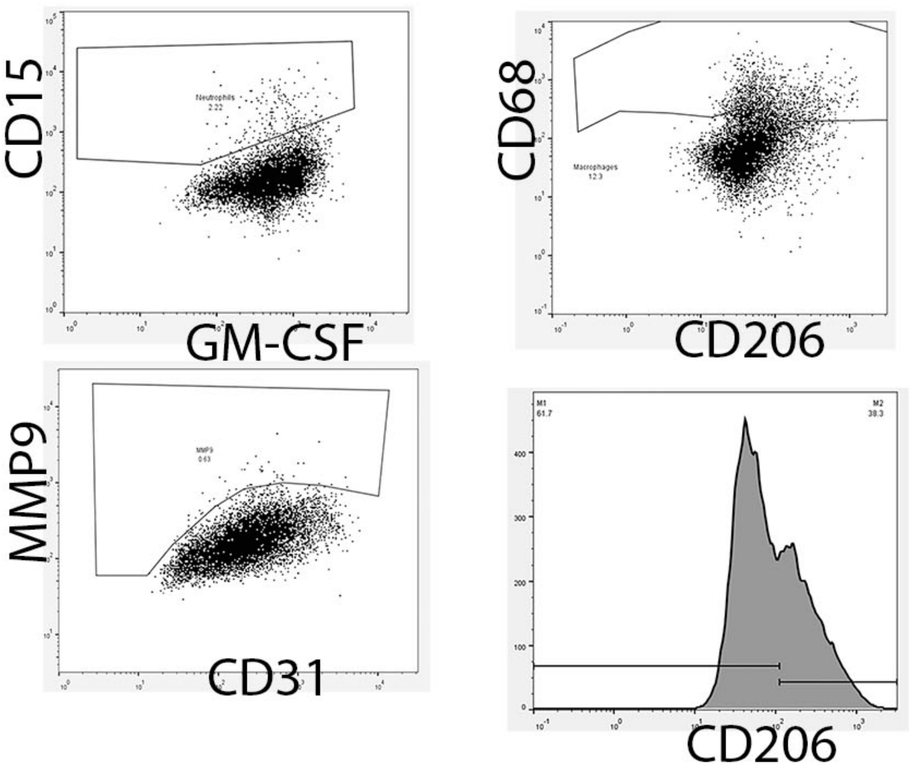

D